© 2019. Published by The Company of Biologists Ltd | Journal of Experimental Biology (2019) 222, jeb208140. doi:10.1242/jeb.208140

RESEARCH ARTICLE

Convergent evolution of super black plumage near bright color in 15 bird families

Dakota E. McCoy[1,*] and Richard O. Prum[2]

ABSTRACT

We examined extremely low-reflectance, velvety black plumage patches in 32 bird species from 15 families and five orders and compared them with 22 closely related control species with normal black plumage. We used scanning electron microscopy to investigate microscopic feather anatomy, and applied spectrophotometry and hyperspectral imaging to measure plumage reflectance. Super black plumages are significantly darker and have more broadband low reflectance than normal black plumages, and they have evolved convergently in 15 avian families. Super black feather barbules quantitatively differ in microstructure from normal black feathers. Microstructural variation is significantly correlated with reflectance: tightly packed, strap-shaped barbules have lower reflectance. We assigned these super black feathers to five heuristic classes of microstructure, each of which has evolved multiple times independently. All classes have minimal exposed horizontal surface area and 3D micrometer-scale cavities greater in width and depth than wavelengths of light. In many species, barbule morphology varied between the super black exposed tip of a feather and its (i) concealed base or (ii) iridescently colored spot. We propose that super black plumages reduce reflectance, and flatten reflectance spectra, through multiple light scattering between the vertically oriented surfaces of microscale cavities, contributing to near-complete absorption of light by melanin. All super black plumage patches identified occur adjacent to brilliant colored patches. Super black plumage lacks all white specular reflections (reference points used to calibrate color perception), thus exaggerating the perceived brightness of nearby colors. We hypothesize that this sensory bias is an unavoidable by-product of color correction in variable light environments.

KEY WORDS: Color correction, Anti-reflection, Reflectance, Sexual selection, Structural absorption, Sensory bias

INTRODUCTION

The physics, chemistry, social function and evolutionary history of avian plumage coloration have been intensively studied, resulting in a deep understanding of the great diversity in the form and function of avian plumage coloration (Hill and McGraw, 2006). For example, birds-of-paradise have evolved sparkling, multicolored, three-dimensional microscopic reflectors (Stavenga et al., 2011; Wilts et al., 2014), an array of elaborate courtship dances (Scholes, 2008; Scholes and Laman, 2018) and spreadable capes of velvet black feathers (Frith and Frith, 1988; McCoy et al., 2018; Scholes and Laman, 2018). Integumentary colors are generally categorized as pigmentary – produced by chemical pigments with specific absorption spectra – or structural – produced by nanoscale features that constructively or destructively interfere with different wavelengths of light. Granules of the pigment melanin, which have a high refractive index, can contribute to structural colors by their packaging and arrangement within the feather (Prum, 2006; Stavenga et al., 2015). This is frequently studied at the nanoscale.

However, microscale morphological features at a larger size scale than wavelengths of light can also impact plumage appearance. Barb and barbule shape, smoothness and orientation can produce glossy features in a diversity of birds (Harvey et al., 2013; Iskandar et al., 2016; Shawkey and D'Alba, 2017). Recently, we have demonstrated that microscale optical cavities in the surface of bird-of-paradise feathers create structurally assisted light absorption – or super black – through multiple scattering (McCoy et al., 2018). As in profoundly black technologies, such as Vantablack™ and carbon nanotube forests, multiple scattering and absorption interact to generate a deep black appearance (Liu et al., 2014). This 'super black' appears to interact with the perceptual mechanisms of the observer to create a distinct sensory experience: an optical illusion that enhances nearby color (Kreezer, 1930; Brainard et al., 1993; Speigle and Brainard, 1996).

Super black plumages in birds-of-paradise (McCoy et al., 2018), super black cuticle in peacock spiders (McCoy et al., 2019) and super black scales in various butterflies (Vukusic et al., 2004) eliminate specular reflections, or white highlights. In all three cases, these super black patches are found adjacent to bright, saturated color patches. Vertebrates use specular highlights to white-balance their visual perceptions and control for variations in the amount and color of ambient light in the visual scene. By reducing specular reflections from super black patches, the adjacent colors in birds-of-paradise, peacock spiders and butterflies may appear brighter or even self-luminous (Brainard et al., 1993; Speigle and Brainard, 1996; Neumeyer et al., 2002; McCoy et al., 2018). This general phenomenon has been confirmed psychologically in humans and goldfish (Neumeyer et al., 2002).

Here, we investigated deep black feathers from 32 species of birds (Fig. 1). We demonstrate that super black plumage has independently evolved in at least 15 different avian families – from eiders (Anatidae) and guans (Cracidae) to hummingbirds (Trochilidae), fairywrens (Maluridae) and fairy-bluebirds (Irenidae). The diverse taxonomic distribution of super black plumage in birds raises important new physical, anatomical and evolutionary questions. How do these feather morphologies absorb ambient light so effectively? How do sexual and social selection for plumage patch brilliance select on the morphology of adjacent black feathers to minimize plumage reflectance?

[1]Department of Organismic and Evolutionary Biology, Harvard University, Cambridge, MA 02138, USA. [2]Department of Ecology and Evolutionary Biology, and Peabody Museum of Natural History, Yale University, New Haven, CT 06520, USA.

*Author for correspondence (dakotamccoy@g.harvard.edu)

D.E.M., 0000-0001-8383-8084

Received 4 June 2019; Accepted 15 August 2019

Journal of Experimental Biology (2019) 222, jeb208140. doi:10.1242/jeb.208140

Fig. 1. Representative species with profoundly dark, super black plumage patches. (A) *Somateria spectabalis*. (B) *Balearica pavonina*. (C) *Oreophasis derbianus*. (D) *Lafresnaya lafresnayi*. (E) *Boissonneaua jardini*. (F) *Philepitta castanea*. (G) *Lepidothrix coronata velutina*. (H) *Malurus melanocephalus*. (I) *Sericulus chrysocephalus*. (J) *Lophorina superba*. (K) *Crypsirina temia*. (L) *Lamprotornis superbus*. (M) *Irena puella*. (N) *Sericossypha albocristata*. (O) *Tangara chilensis*. (P) *Cyanerpes cyaneus*. Photo credits: (A) Ron Knight (CC BY 2.0); (B) Michael Möller (CC BY-SA 2.0 DE); (C) Yinan Chen; (D) Ralph Paonessa; (E) Gaston Cassus; (F) Werner Suter; (G) Photo © 2011 Justin Black/justinblackphoto.com; (H) Greg Miles (CC BY-SA 2.0); (I) Rob Drummond; (J) Ed Scholes; (K) Michael Gillam (CC BY 2.0); (L) Robert Winslow; (M) Bob Barbour, www.BobBarbour.Photoshelter.com; (N) Lou Hegedus; (O) Shane Torgerson; (P) Alexander Ramirez. Photos may not be reproduced without permission from the photographers.

In this study, we investigated the reflectance and morphological structure of super black plumages – defined as having less than 2% directional reflectance at normal incidence, with broadband low reflectance – across Aves. Using spectrophotometry and scanning electron microscopy (SEM), we compared profoundly black patches with normal black plumages from closely related, phylogenetic control species. The profoundly black plumages are significantly darker than normal black plumages. Further, we identified five

Journal of Experimental Biology (2019) 222, jeb208140. doi:10.1242/jeb.208140

anatomical classes of super black barbule morphology, each of which evolved independently in multiple families. A phylogenetic PCA identifies two features which primarily separate super black feathers from normal black feathers: interbarbule distance and strap-shaped (rather than cylindrical) barbules, which are angled perpendicularly to the feather vane. Both features reduce exposed horizontal surface area and provide vertical surfaces that multiply scatter reflected light among feather barbules. We propose that each morphological class functions through structurally assisted absorption to reduce reflectance, as has previously been demonstrated for many manmade materials (Brown et al., 2002; Zhao et al., 2011a; Panagiotopoulos et al., 2012; Liu et al., 2014), birds-of-paradise (McCoy et al., 2018), peacock spiders (McCoy et al., 2019), butterflies (Vukusic et al., 2004), the West African Gaboon viper (Spinner et al., 2013) and a stick insect (Maurer et al., 2017). Structurally assisted absorption, hereafter 'structural absorption', occurs when micro- or nano-structures scatter or diffract light to enhance absorption by a material (Brown et al., 2002; Crouch et al., 2004; Vorobyev et al., 2009; Tao et al., 2012; Liu et al., 2014; McCoy et al., 2019).

In all avian species tested, profoundly black plumage was located adjacent to brilliantly colored plumage patches or fleshy ornaments. We hypothesize that super black plumages have evolved through sensory bias, owing to fundamental features of the cognitive color correction mechanisms in the vertebrate visual system, which exaggerate the perceived brilliance of adjacent colors. The massively convergent evolution of super black plumages in association with bright, saturated color patches in many avian lineages provides further evidence for this generalized sensory bias in color perception.

MATERIALS AND METHODS

Specimens

We selected 32 bird species with profoundly black plumage from 15 families and five orders, and 22 closely related species with normal black plumage for the study (Dataset 1). The species were identified by visual observation of museum study skins from the Yale Peabody Museum (YPM), the Harvard Museum of Comparative Zoology (MCZ) and the American Museum of Natural History (AMNH; Dataset 1). To the human eye, super black plumage patches are strongly velvet with minimal specular reflectance, such that it is difficult to focus on the surface of the plumage. The species with normal black plumage lacked any conspicuous glossy specular highlights, but the surface of the feathers is easily perceived. Individual contour feathers were sampled from museum skins for scanning electron microscopy (SEM). Three species had both super black and normal black patches in the same plumage: *Oreophasis derbianus*, *Lophorina superba* and *Coeligena torquata* (Dataset 1).

Spectrophotometry (reflectance)

Reflectance spectra were recorded directly from plumage patches on prepared museum skins. Directional reflectance spectra between 300 and 700 nm were measured perpendicular to the plumage with an Ocean Optics USB2000 spectrophotometer with a bifurcated probe and Ocean Optics DH-2000Bal deuterium-halogen light source. Spectralon (Ocean Optics) was used as a white standard. Negative values recorded for some measures of super black plumage were converted to 0, and three spectra from each patch (different locations within the patch) were averaged to produce an average spectrum for the patch (five for birds-of-paradise; McCoy et al., 2018). Two specimens per species were measured for all species except seven for which only one specimen was available (Dataset 1). To produce final reflectance curves (Fig. S1), we averaged values from both specimens. Reflectance was calculated as the area under the measured reflectance spectrum by integrating the LOESS (locally estimated scatterplot smoothing) curve between 300 and 700 nm, then dividing that value by the integral of a 100% reflectance curve (the white standard).

Many species retain a profoundly black appearance after gold coating for SEM, which demonstrates a structural component to the black color. In order to quantify how dark these feathers were after being coated in gold (i.e. to quantify the structural contribution), we used hyperspectral imaging for two species, *Drepanornis bruijnii* and *Lamprotornis splendidus*. Specifically, we used a form of microspectrophotometry that captures an image where every pixel encodes a reflectance spectrum between wavelengths 420 and 1000 nm, normalized by a mirror standard (Thorlabs Inc.). We used a Horiba and Cytoviva Model XploRA Hyperspectral Microscope with MicroManager and ENVI software (issue 4.8). The light source was a DC-950 Fiber-Lite (Colan-Jenner Industries). We used a 50× microscope objective (numerical aperture 0.5) and exposure time of 1000 ms for the super black regions. The mirror standard was too reflective for this exposure time, so we used an exposure of 100 ms and multiplied all values by 10 (we could perform a linear transformation because the charged coupled device is a linear detector for the intensities employed). To control for background noise from our instruments, we normalized all measurements by the lamp spectrum; to ensure there was no background noise from ambient conditions, we turned off the light source and took a hyperspectral measurement. From the resulting hyperspectral images, we averaged 10 reflectance spectra. To calculate total percent reflectance, we integrated a LOESS curve from wavelengths 420–700 nm and divided the result by the integral of a perfect mirror reflectance standard with reflectance=100% for the studied 280 nm wavelength span.

Lastly, we calculated the 'flatness' of the reflectance spectra of super black and normal black birds, by fitting a linear model to the reflectance spectra, and recording the slope. In this manner, we can compare the rise in reflectance over the avian visual spectrum between normal and super black plumages.

To create phylogenetically independent comparisons of reflectance and slope between super black feathers and normal black feathers, we paired super black species with a closely related normal black bird, a phylogenetic 'control' species from within the same, or nearest, family (see Dataset 1). Because super black plumage is not a homologous character shared among multiple bird families (see below), each such comparison constitutes a phylogenetically independent comparison (*sensu* Felsenstein, 1985). We then performed a paired two-sided *t*-test in R version 3.4.3 with these phylogenetically controlled species pairs, randomly selecting one super black and one control species per family group. We repeated this procedure with 100 random selections of control and test pairs to check for robustness and ensure that our random choice of control and test birds did not impact results.

Scanning electron microscopy (microstructure)

For SEM, feathers were mounted on stubs using carbon adhesive tabs, coated with ∼15 nm of gold or platinum/palladium, and viewed and micrographed using an ISI SS40 SEM operating at 10 kV or an SEM-4 FESEM Ultra55 operating at 5 kV. All SEM figures are available from the corresponding author upon request.

To quantify feather microstructure, we measured nine barbule features on each species (we took 10 measurements for each feature in ImageJ and averaged them). These are 2D measurements of a 2D representation of a 3D structure, but they nonetheless are a useful

start to understanding qualitative categories of barbule microstructure. The two species categorized as 'brushy barb' (*O. derbianus* and *Somateria fischeri*) were excluded from the phylogenetic PCA analysis because they do not have barbules.

Variables included: (1) barb/barbule angle, the angle between the barbules and the central barb; (2) barbule length, the full length of the barbule, following the path of the barbule free-hand; (3) barbule thickness, the thickness of the barbule viewed from the side (i.e. thinnest point); (4) barbule width, the width of the barbule viewed head-on (i.e. widest point); (5) central barb width, the width of the central barb viewed top-down; (6) degree of barbule curvature, where a circle was fit to the curviest portion of each barbule (in many cases, the entire barbule curved smoothly) and the diameter of curvature was recorded, the arc length of the curved portion was also recorded, and from this the degree of curvature was calculated; (7) inter-barbule distance, the distance between two adjacent barbules on one side of a feather; (8) length of marginal spikes, the length of spikes, approximated by a straight light running from tip of spike along the center of the spike to marginal edge of the barbule; and (9) strappiness, barbule width divided by thickness.

Phylogenetic analyses

To perform robust phylogenetic analyses (Jetz et al., 2012, 2014; Rubolini et al., 2015), we downloaded 100 trees from birdtree.org, including all species measured herein and in Stoddard and Prum (2011).

For phylogenetically controlled principal component analysis (phyloPCA) of feather microstructural characters, we scaled and centered all data before the analysis and then used function phyl.pca in the R package phytools (Revell, 2012). For the method of correlation, we used lambda, and the PCA mode was set to 'cov' (covariance).

We performed a phylogenetic generalized least squares (PGLS) model to test for correlations between feather microstructure and percent reflectance. We used the PCA PC1 scores, which captured 33.3% of the variance in feather microstructure. We used PGLS (Grafen, 1989; Martins and Hansen, 1997) with a Brownian motion model to account for phylogeny. We repeated this analysis for 100 phylogenetic trees (first calculating PC1, then fitting a PGLS model) and recorded estimates, 95% confidence intervals and *P*-values for all. PGLS is required rather than a non-phylogenetic method even though we are using phylogenetic PCA scores (Revell, 2009).

We reconstructed the evolutionary history of black plumage reflectance for a large sample of avian species, both those measured herein and those measured in the eumelanin spectral archive (Stoddard and Prum, 2011). We removed species with reflectance >10% from Stoddard and Prum (2011). We performed the reconstruction with the contMap function in phytools v. 0.6-44 (Revell, 2012, 2013), which uses maximum likelihood to estimate states at internal nodes and interpolate these states along internal branches (Felsenstein, 1985). We performed this analysis on a consensus tree, obtained through the function consensus.edges in the library phytools in R.

RESULTS

Reflectance

We compared super black plumages – which are all, except for one, adjacent to saturated color patches (Fig. 1) – with normal black plumages. Super black plumages were profoundly darker, with flatter reflectance curves, than normal black plumages (Figs 2 and 3). Reflectance of the super black plumages ranged from 0.045% (*Astrapia stephaniae*) to 1.97% (*Malurus alboscapulatus*) and averaged 0.94%. For the control black birds, reflectance ranged from 2.32% to 6.26% and averaged 4.02%.

Super black plumages reflected significantly less light than did normal black plumages of phylogenetic control species for reflectance with 90 deg incident light (paired *t*-tests: $P<0.0005$; 95% CI=−0.038, −0.025; Figs 2 and 3A, Fig. S1). Statistics are presented for one randomly chosen control and super black bird per family. We repeated the test procedure 100 times with randomly selected pairs of super black and control species for families with multiple samples of either, and found significant results irrespective of which super black and control birds were chosen in each family (average *P*-value=8.25×10^{-8}, average 95% CI=−0.039, −0.026; for distributions of *P*-values and confidence intervals, see Fig. S2A,B).

As predicted, reflectance spectra of super black bird plumages were nearly flat compared with normal black plumages, whereas reflectance spectra of normal black plumages showed pronounced upward slopes at longer wavelengths (Figs 2 and 3C, Fig. S1). Surface structure can enhance the absorption efficiency of melanin by multiply scattering light among 3D elements of the feather. With each scattering event, some proportion of incident light is transmitted and absorbed (Brown et al., 2002; Crouch et al., 2004; Vorobyev et al., 2009; Tao et al., 2012; Liu et al., 2014). By iterative absorption, these plumages achieve a super black, broadband appearance.

For reflectance spectra, control birds had slopes ranging from 0.24 to 10 with a mean of 5.3% μm^{-1}, while super black birds ranged from 0.16 to 3.5 with a mean of 1.1% μm^{-1}). The slopes of super black reflectance spectra were significantly lower (i.e. the spectra were flatter) than those of normal black plumages (paired *t*-tests: $P<0.0005$; 95% CI=−6.0, −3.4; Fig. 3C,D). Statistics are presented for one randomly chosen control and super black bird per family. We repeated the test procedure 100 times with randomly selected pairs of super black and control species for families with multiple samples of either, and found significant results irrespective of which super black and control birds were chosen in each family (average *P*-value=2.0×10^{-5}, average 95% CI=−5.6, −2.8; for distributions of *P*-values and confidence intervals, see Fig. S2C,D).

In many cases, as predicted by iterative absorption, super black plumages had reflectance curves with a spectral shape similar to that of normal black plumage reflectance curves of their closest relative divided by a factor of 3–12 (depending on the species). This proportionality factor differs substantially between families, for example, ranging from ∼3–4 in Trochilidae and Pipridae to ∼8 in Gruidae and ∼10–12 in Cnemophilidae and Paradisaeidae. Intriguingly, for several taxa, the super black curves do not show a proportional rise in reflectance (i.e. super black curves appear substantially flatter even when divided by an appropriate proportionality factor). These taxa are *Malurus* spp., some birds-of-paradise (Paradiseaidae), *Irena puella* and *Nettapus auritus*. All except *Malurus* spp. have curved array barbules, the most efficient microstructural enhancers of absorption reported here.

Black plumages measured herein were combined with a previous study of 134 black, eumelanin pigmented plumage patches from 53 species of birds (Stoddard and Prum, 2011) to achieve representation among 40 total avian families (Fig. 3B,D). An ancestral state reconstruction illustrates that the ancestral state of black plumage reflectance is highly likely to be ≥4% reflectance (Fig. 4). We document at least 15 independent evolutionary origins of super black plumage in 15 families. Super black, defined as less than 2% reflectance, evolved from ancestral states of 3–5% reflectance.

To show how dark and broadband low reflection these plumages are in the larger context of bird plumage diversity, we also plotted

Journal of Experimental Biology (2019) 222, jeb208140. doi:10.1242/jeb.208140

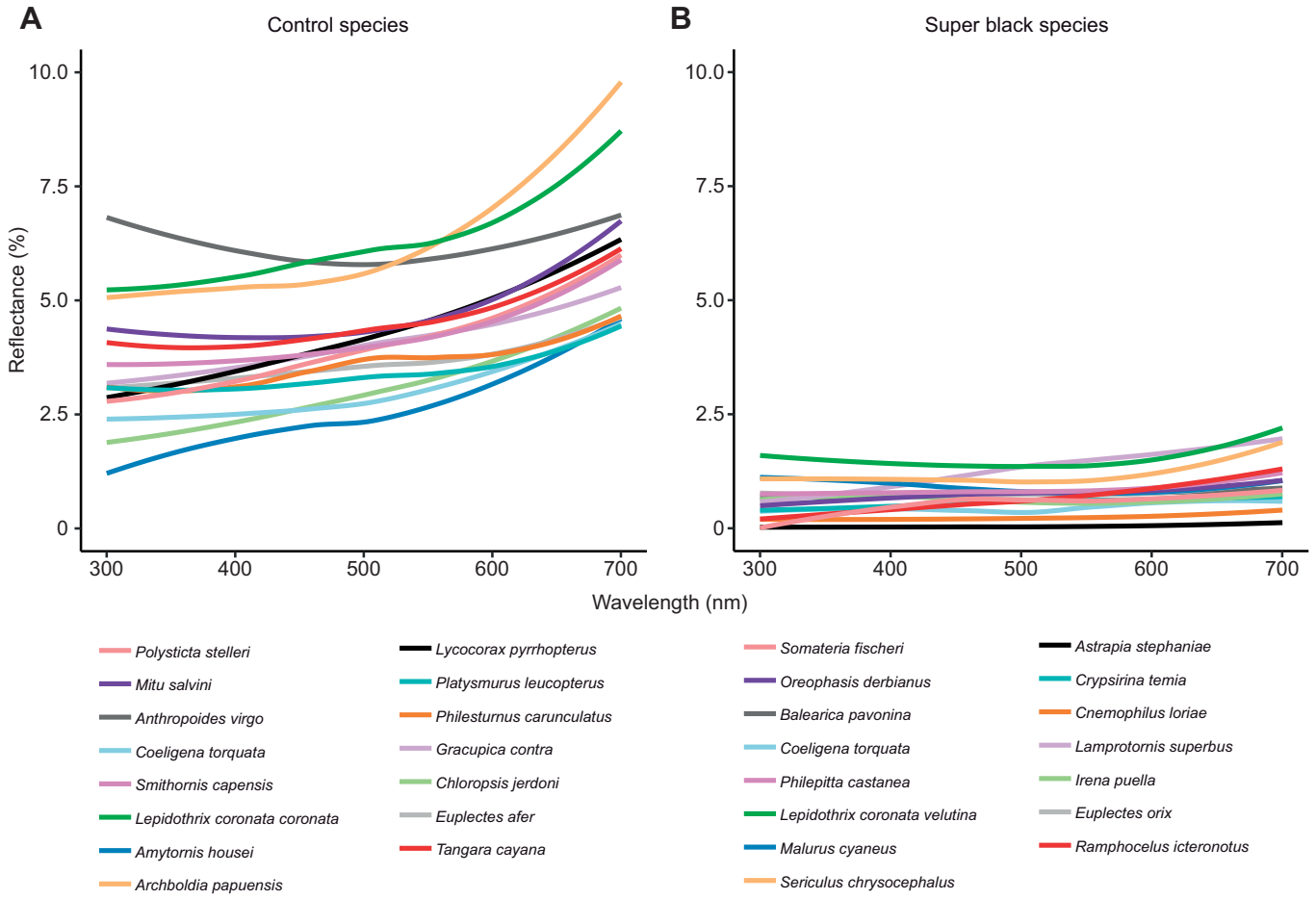

Fig. 2. Super black plumage has low, broadband reflectance. (A) Control species with normal black plumage. (B) Sample species with super black plumage (structurally assisted absorption). Here, we plot *n*=30 example species; plumage patch locations and percent reflectance for all species are in Dataset 1; all reflectance curves are in Fig. S1.

the total reflectance and slope of the reflectance spectrum from the Stoddard and Prum (2011) dataset (Fig. 3B,D) after eliminating patches from this previous sample that had more than 10% reflectance. Of the remaining 120 plumage patches, the mean reflectance was 3.95%, and the mean reflectance spectrum slope was 4.0% μm^{-1} (values comparable to those of the normal, control black birds chosen in this study).

We observed that every instance but one of super black plumage was associated with a brilliant and highly chromatic plumage color patch (Dataset 1), or a fleshy patch, horn or caruncle (*Somateria spectabalis*, *O. derbianus*, *Balearica pavonina*, *Philepitta castanea*). Control species with normal black plumage had few colorful patches (Dataset 1). White patches, however, were observed in multiple control species, but only one of the super black species had an adjacent white patch (Dataset 1; see Discussion, Super black occurs near brilliant color in visual displays).

Remarkably, some super black feathers still appear profoundly black even after being coated in ∼15 nm gold for SEM. We measured the reflectances of two feathers that appeared black even with a gold coating, an upper wing covert from *L. splendidus* and a pectoral plume from *D. bruinjii*, using a microscope equipped with hyperspectral imaging. Typically, feathers coated in gold appear gold; indeed, the bright, structurally colored regions of the gold-coated *D. bruinjii* feather reflected between 10 and 20% of light across all wavelengths (Fig. S3). In contrast, in both cases, reflectance of the gold coated super black region was <0.5% across all measured wavelengths – two orders of magnitude lower (Fig. S3). These data provide strong physical evidence for structural absorption.

Feather morphology

Our evaluation of SEMs of feathers from super black plumage patches from 15 different families revealed multiple qualitative differences of barbule morphology that we classified heuristically in five classes (Fig. 5). Each of these barbule types has evolved in at least two families separately (Fig. 4). Furthermore, we made quantitative measurements of SEMs from all feathers and documented clustering by morphological group (Fig. 6A).

SEMs of normal black plumage patches revealed uniform barbule structure and cluster together in the phylogenetic PCA (Fig. 6A, Figs S4–S6): the barbules are simple, undifferentiated and generally oriented horizontally (the only exception being *Tangara cayana*, for which barbules demonstrate some vertical angling; Fig. S6D). Very little variation in barbule morphology was observed between the exposed distal and more basal portions of the feather vane or an individual barb.

In contrast, super black feathers cluster separately from the normal black feathers on the phylogenetic PCA (Fig. 6A); they produce multiple scattering and enhanced melanin absorption through a variety of three-dimensional surface structures (Fig. 5,

Journal of Experimental Biology (2019) 222, jeb208140. doi:10.1242/jeb.208140

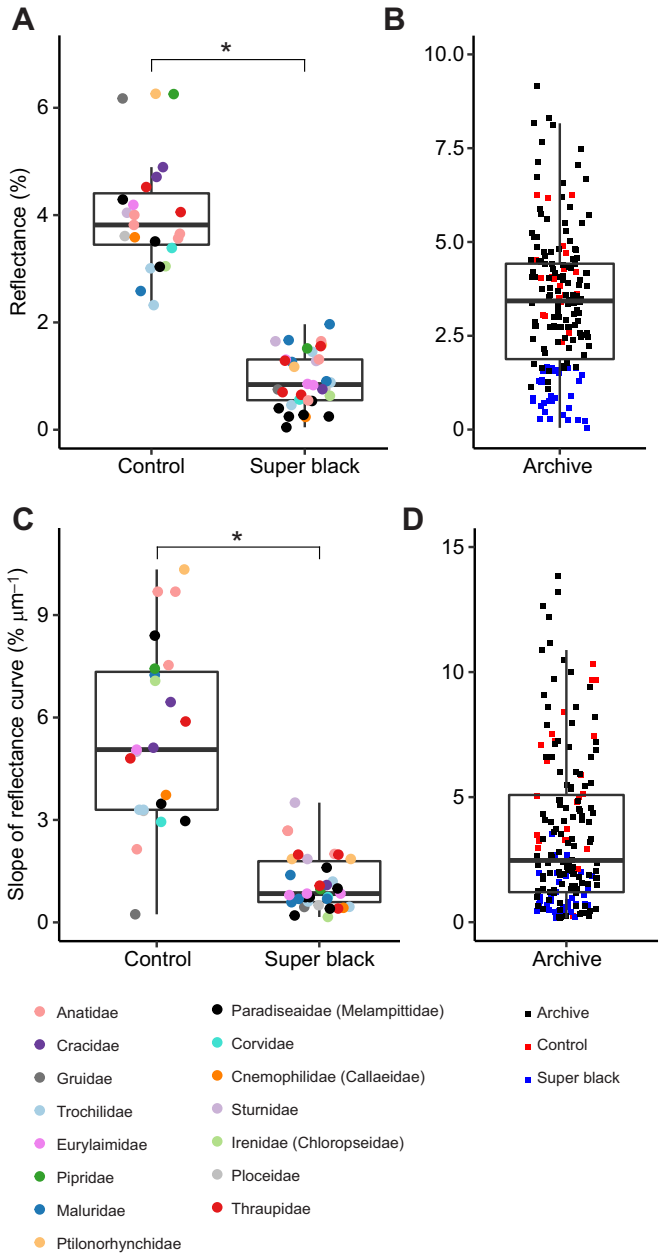

Fig. 3. Super black plumage is significantly darker, with a flatter reflectance curve, than normal black plumage. (A) Percent reflectance, 90 deg incident light, for n=55 control and super black birds; P<0.0005; 95% CI=−0.040, −0.023. (B) Percent reflectance, 90 deg incident light, from an archive of n=120 black plumage patches from 53 bird species (Stoddard and Prum, 2011) with all control (green) and super black species (purple) plotted. (C) Slope of linear model of the reflectance spectra for n=55 control and super black birds; P<0.0005; 95% CI=−6.0, −3.4. The outlier among control bird slopes (dark grey dot) is *Anthropoides virgo* (Gruidae), which has a U-shaped reflectance curve (i.e. slope of linear fit is near 0) but still reflects 5–7% of light; see Fig. 2A. (D) Slope of linear models of reflectance curves from an archive of n=120 black plumage patches from 53 bird species (Stoddard and Prum, 2011) with all control (green) and super black species (purple) plotted. Statistics are presented for one randomly chosen control and super black bird per family; details in Materials and Methods. All P-values and confidence intervals from the 100 repetitions are plotted in Fig. S2A–D.

Figs S4–S6). We identified five qualitative categories of super black plumages: (1) curved arrays, (2) dihedral straps, (3) dense straps, (4) sparse straps and (5) brushy barbs.

Curved arrays (dense, curved, upright array of barbules)

Eleven species from five families showed densely packed barbules that curve vertically above the plane of the feather vane at variable angles (Fig. 5A,B). Species with this morphology are six birds-of-paradise, *Ptiloris paradiseus*, *A. stephaniae*, *Seleucidis melanoleucus*, *Parotia wahnesi*, *D. bruijnii* and *L. superba* (Paradiseaidae; all but *D. bruijnii* previously reported in McCoy et al., 2018); the Asian fairy-bluebird, *I. puella* (Irenidae); two starlings, *Lamprotornis superbus* and *L. splendidus* (Sturnidae); the duck *Nettapus auratus* (Anatidae); and the velvet satinbird, *Cnemophilus loriae* (Cnemophilidae) (Figs 5A,B, 6A, 7A). These structures form a disorganized array of curved, planar structures sticking up from the barb ramus like a semi-cylindrical bottle brush. The barbules of the birds-of-paradise, *C. loriae* and *I. puella* have spikes and protrusions along their margins, like serrations on leaves. The starlings *L. superbus* and *L. splendidus* have largely smooth, undifferentiated barbule margins; occasionally, some marginal spikes and protrusions are visible (Fig. 5A). The curvature of the barbule surfaces creates complex microcavities between barbules, in which straight-line paths out of the bottom of the cavity are limited or nonexistent. We note that *N. auratus* and *C. loriae* combine this barbule morphology in a dihedral organization (see below).

Dihedral straps (dense, strap-shaped, dihedral barbules)

Six species from five families have densely packed, strap-shaped barbules that angle upwards toward the upper (obverse) surface of the feather vane on either side of the ramus to form a dihedrally shaped vanule, or ‘valley’, toward the tip of each ramus (Figs 5C,D, 6A, 7B). These species with dihedral morphology are the crane *B. pavonina* (Gruidae); the bowerbirds *Sericulus chrysocephalus* and *S. bakeri* (Ptilonorhynchidae); and the tanager *Ramphocelus icteronotus* (Thraupidae). The barbules are simple and rectangular in cross-section, with minimal change in barbule shape from base to tip. The barbules are quite straight (*S. chrysocephalus*) or only slightly curved (*R. icteronotus*), and oriented parallel to one another. Barbules extend from the rami in neat rows at a constant angle without radial dissymmetry. The barb itself is extremely oblong, shaped like a razor rather than a cylinder, with a minimum of horizontally exposed surface area. The duck *N. auratus* (Anatidae) and the velvet satinbird, *C. loriae* (Cnemophilidae), combine the dihedral organization with curved barbule surfaces and complex protrusions on the barbule margins (see above).

Dense straps (dense, bundled, strap-like or hair-like barbules)

Eight species from five families have densely spaced, strap-like barbules with generally simple margins that curve only slightly upwards, most notably toward the end of each ramus where the barbules appear ‘bundled’ or ‘hairlike’ (Figs 5E,F, 6A, 7C). The strap-shaped barbules are oriented with their narrow margins facing outward (obverse) and their broad surfaces facing one another, in the plane of the vane. Species with these feathers are the broadbill *P. castanea* (Eurylaimidae); two fairywrens, *Malurus cyaneus* and *M. melanocephalus* (Maluridae); the treepie *Crypsirina temia* (Corvidae); the bishop *Euplectes orix* (Ploceidae); and three tanagers, *Cyanerpes cyaneus*, *Sericossypha albocristata* and *Tangara chilensis* (Thraupidae). The barbules are not oriented in neat rows, like they are in the ‘dihedral strap’ species, but appear more chaotic (like branches of pine trees). However, the barbules are similarly simple and rectangular in structure.

Sparse straps (sparse, strap-shaped barbules)

Six species from four families have vertically oriented, strap-shaped barbules (i.e. higher than they are wide) with a minimum of

Journal of Experimental Biology (2019) 222, jeb208140. doi:10.1242/jeb.208140

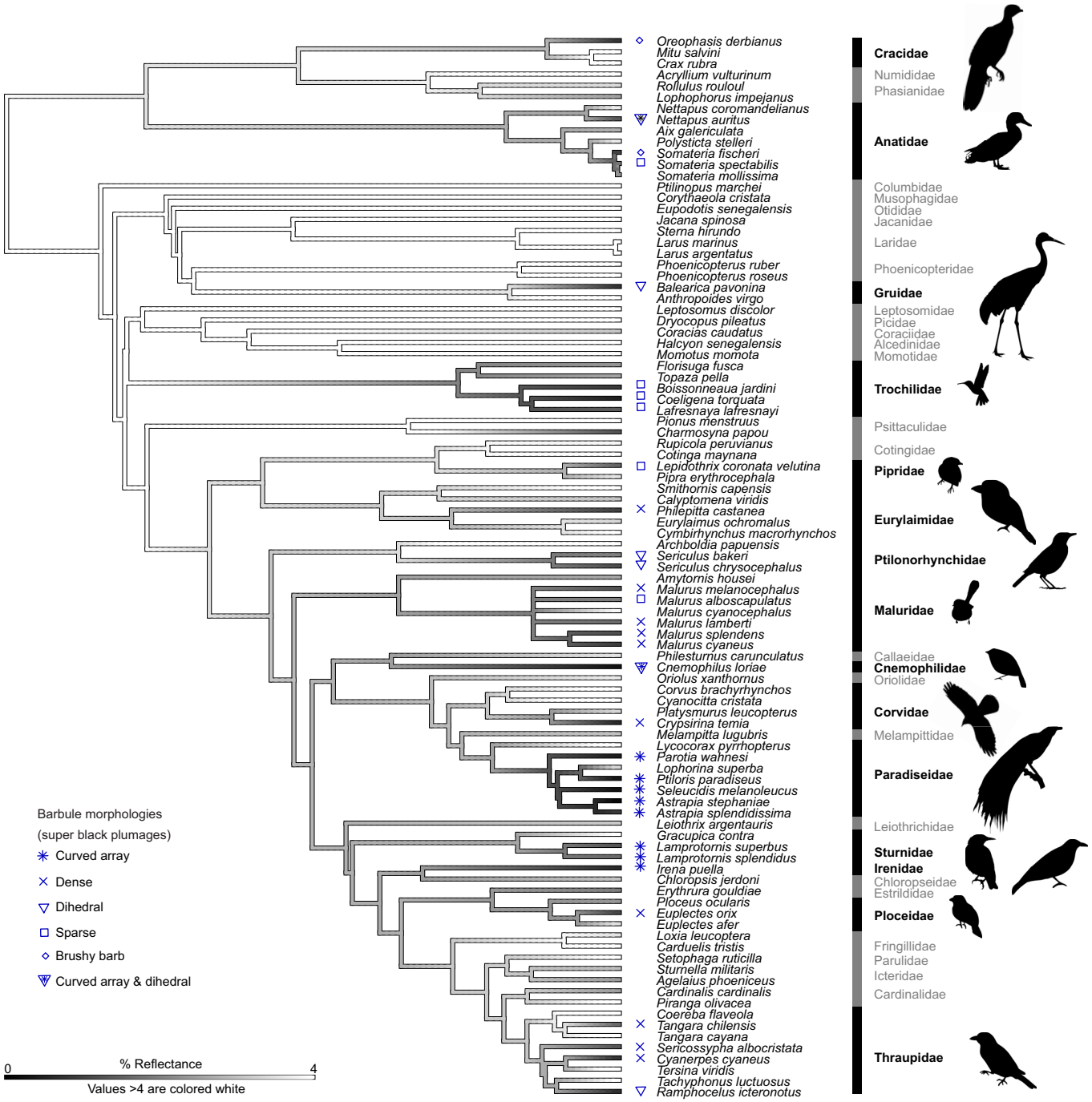

Fig. 4. Super black plumage has evolved independently in at least 15 avian families. An ancestral state reconstruction of reflectance is presented on a consensus phylogenetic tree to illustrate the multiple parallel evolutions of super black in 15 avian families. Reflectance data from this paper were combined with data from Stoddard and Prum (2011). Families are listed on the right, and families with at least one evolution of super black are written in black rather than grey with an accompanying silhouette. *Lepidothrix coronata* refers to subspecies *velutina*; subspecies *coronata* is not included here. *Drepanornis bruinjii* had no available phylogenetic data and is not included. Silhouette credits (from Phylopic.org): Cracidae: uncredited, copyright free; Anatidae: Maija Karala; Gruidae: Lauren Anderson; Trochilidae, Ptilonorhyncidae, Paradiseidae: Ferran Sayol; Corvidae: L. Shyamal; Maluridae: Michael Scroggie; Sturnidae: Maxime Dahirel. We generated silhouettes for Pipridae, Eurylaimidae, Cnemophilidae, Ploceidae, Irenidae and Thraupidae.

broad, horizontally exposed surfaces (Figs 5G,H, 6A, 7D). Species with the sparse strap morphology are the duck *Somateria spectabilis* (Anatidae), the hummingbirds *C. torquata* (nape), *Boissonneaua jardini* and *Lafresnaya lafresnayi* (Trochilidae), the manakin *Lepidothrix coronata velutina* (Pipridae) and the Australasian wren *M. alboscapulatus* (Maluridae). The flat surfaces of the barbules are slightly twisted near the base (thus exposing some horizontal surface), but at the tip almost no surface is horizontally exposed. These barbules are not densely packed near each other on the ramus; however, observations of the specimens suggest that the feathers themselves are densely packed.

Journal of Experimental Biology (2019) 222, jeb208140. doi:10.1242/jeb.208140

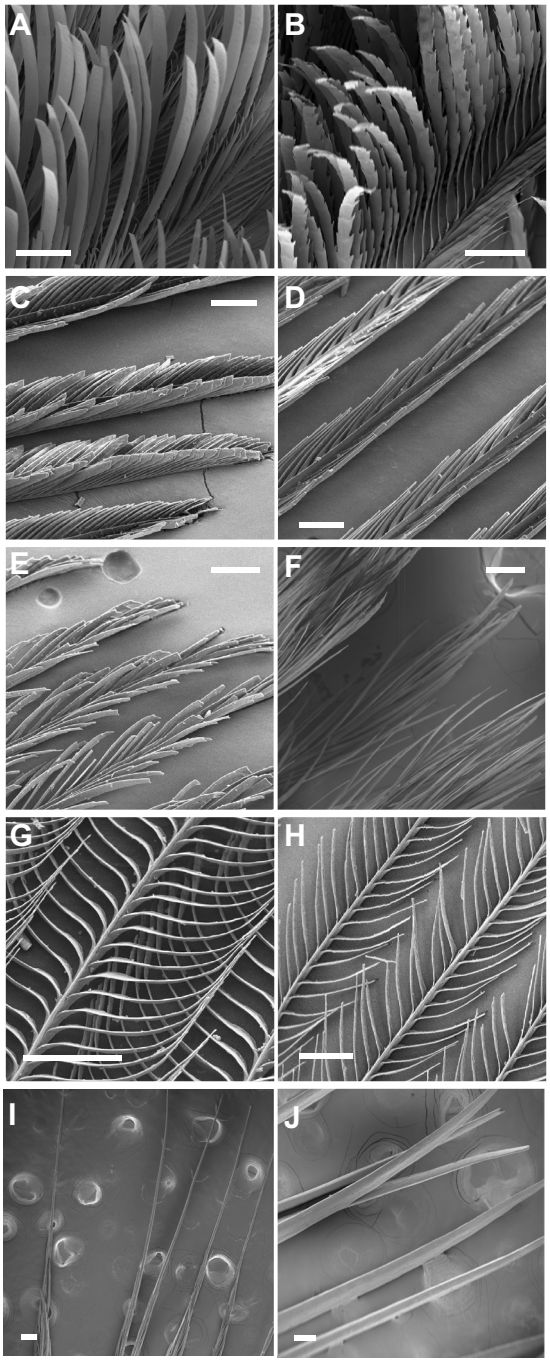

Fig. 5. Birds evolved five morphological categories of super black feathers with structurally assisted absorption. We observed five qualitative categories of feathers (for quantitative analysis, see Fig. 6) based on barbule morphology: (A,B) curved arrays, (C,D) dihedral straps, (E,F) dense straps, (G,H) sparse straps and (I,J) brushy barbs. (A) *Lamprotornis superbus* black spot on wing covert; (B) *Drepanornis bruijnii* black spot on pectoral plume; (C) *Ramphocelus icteronotus* back; (D) *Sericulus chrysocephalus* back; (E) *Tangara chilensis* back; (F) *Malurus cyaneus* upper back; (G) *Boissonneaua jardini*; (H) *Somateria spectabilis* rim around bill; (I) *Oreophasis derbianus* forecrown; (J) *Somateria fischeri* facial ring. Scale bars are 100 µm.

Brushy barbs (no barbules at tip, narrow tapered barbs)

Black feathers from the horned guan, *O. derbianus*, forecrown and the duck *S. fischeri* eyering are very tiny, erect and completely lack barbules at the tip (Figs 5I,J, 6A, 7E, Fig. S4A,B). The barbs are long and tapering. This very simple morphology suggests that scattering interactions among multiple feathers play an important role in structural absorption in these plumages.

Phylogenetic PCA

The phylogenetic PCA supported three distinct feather groups primarily along PC1: control feathers at one end, curved array super black feathers at the other end, and all other super black feathers in between. PC1 was correlated with (i) the extent to which barbules are strap-shaped versus cylindrical and (ii) the distance between barbules (Fig. 6A, Dataset 2). These are two proxies for exposed horizontal surface area. The most strap-shaped and most tightly packed barbules are curved arrays, while at the other end are the control feathers. In between is a cluster of feathers with strap-shaped barbules that we divide into dihedral, dense and sparse based on additional qualitative characteristics that were not distinguished by the PCA. Brushy barb feathers were not included in the PCA because they have no barbules.

Morphology and reflectance variation among feather classes

PC1, a measure of feather microstructure, is significantly correlated with reflectance (PGLS; for one tree, estimate=−0.30, 95% CI=−0.47, −0.14, $P<0.005$; Fig. 6B; P-values and confidence intervals for the same analysis conducted over 100 trees are presented in Fig. S2E,F; results were significant in each case). In other words, feathers with more strap-shaped (rather than cylindrical) barbules, and with more tightly packed barbules, are darker. This analysis was conducted without the brushy barb class feathers, which do not have barbules.

The five morphological classes varied substantially in their absorption efficiency (Fig. 6B). The darkest two classes were curved array and brushy barbs, with mean reflectances of 0.58% and 0.62%, respectively. The other three morphological classes had mean reflectance values closer to 1%: dihedral strap (0.88%), dense strap (1.03%) and sparse strap (mean 1.25%). We ranked these barbule classes and ‘normal’ class from 1 to 6, with 1 through 5 being those five super black morphologies and 6 being the control feathers, and applied a tie-corrected Spearman’s rank correlation in R (version 3.4.3 2017). We found Spearman’s rho=0.85, $P<0.0005$ (this result was robust when we applied Kendall’s tau-B as well).

Within-feather variation in morphology

In most species, it was also possible to identify barbule morphologies associated with light absorption by comparing barbules at the exposed distal tips of the feather vane with those nearer the bases of the feather vane (McCoy et al., 2018), because the exposed tips of the vanes contribute to the plumage appearance while the bases of the vanes are concealed within the plumage by other, overlying contour feathers.

Philepitta castanea provides an interesting exception. At the end of the breeding season, male *P. castanea* have a single, annual, prebasic molt that produces a plumage with a scaly appearance of contour feathers with yellow-green distal tips and black bases (Prum and Razafindratsita, 1997). Over the non-breeding season, the green tips gradually wear off to reveal a distinctive, super black male breeding aspect, which gives the velvet asity its common name. The green tips of the freshly molted male contour feathers have carotenoid pigments and relatively sparse barbules that form a flat, horizontal vanule. However, toward the bases of these feathers, the melanin pigmented barbules, which will be fully exposed after feather wear during the breeding season, are much denser and exhibit the prominent dihedral vanules.

Journal of Experimental Biology (2019) 222, jeb208140. doi:10.1242/jeb.208140

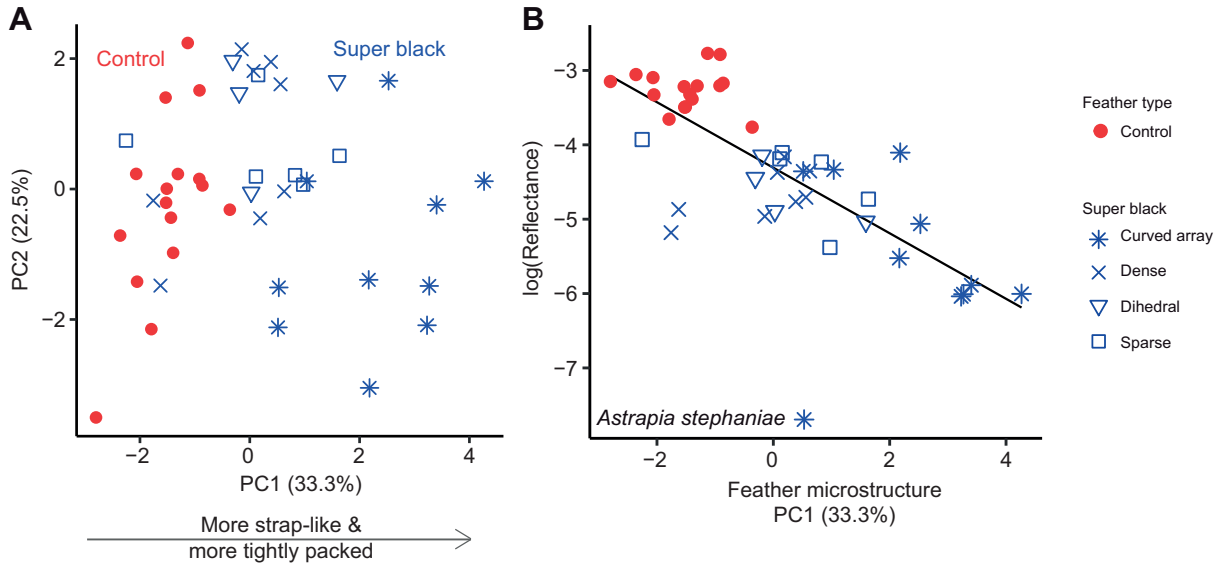

Fig. 6. Feather barbule microstructure is significantly correlated with reflectance. We included *n*=53 species; brushy barb feathers are not included here, because they have no barbules. (A) A phylogenetic PCA reveals that feathers cluster into discrete morphological groups based on microstructural measurements (for PCA loadings and PCA scores by species, see Dataset 2); PC1 scores were determined primarily by how much exposed surface area was present on the feathers (how strap-shaped barbules were and inter-barbule distance), while PC2 was largely determined by barb/barbule angle and degree of curvature. The two species categorized as 'brushy barb' (*Oreophasis derbianus* and *Somateria fischeri*) were excluded from the phylogenetic PCA analysis because they do not have barbules. (B) PC1, a measure of feather microstructure, is significantly correlated with log(reflectance) (PGLS; for one tree, estimate=−0.30, 95% CI=−0.46, −0.14, *P*<0.005; Fig. 6B; *P*-values and confidence intervals for same analysis conducted over 100 trees are presented in Fig. S2E,F). We repeated the phylogenetic PCA and the PGLS model over 100 trees; *P*-values and confidence intervals for all analyses are presented in Fig. S2E,F.

In three species, barbule morphology varied significantly within a single feather between areas of structural black and vivid structurally color, which are produced by arrays of melanosomes within the barbules (Fig. 8). *Lamprotornis superbus* and *L. splendidus* have black spots on their wing covert feathers that are surrounded by iridescent blue. *Drepanornis bruijnii* has black pectoral plumes tipped with structural red or blue. In all three species, barbules within the iridescent portions of the vane were flat, smooth, straps lying horizontal in the plane of the feather, but in the super black areas, the barbules curved conspicuously upwards and gained some jagged tips to their margins (Fig. 8).

DISCUSSION

Super black plumage evolved convergently in 15 avian families

Here, we describe the convergent evolution of super black plumage in 15 families of birds from five orders (Figs 1 and 4). These species have less than 2% reflectance of directly incident light. Super black is defined as a structural or structurally assisted black surface with (i) significantly reduced specular reflectance and (ii) a flatter reflectance curve (broadband low-reflectance) compared with that expected from a flat surface of the same material (Zhao et al., 2011a; Panagiotopoulos et al., 2012; McCoy et al., 2018). The super black plumages described here are significantly

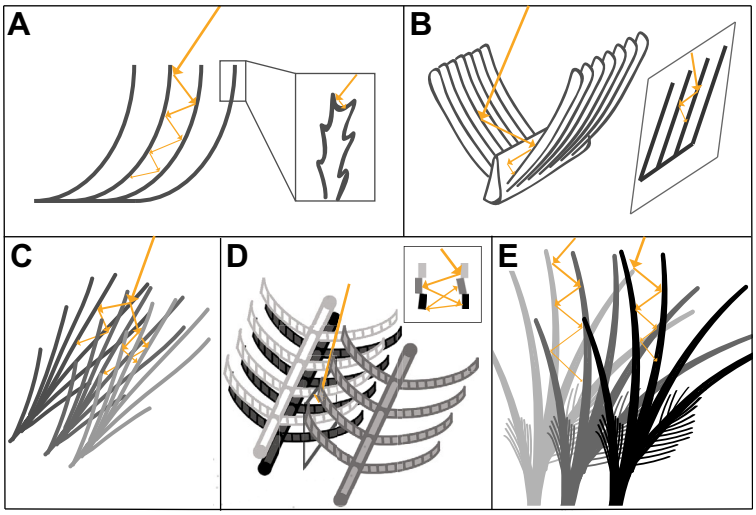

Fig. 7. Schematic models of structural absorption for each of five feather morphology classes. (A) Curved array feathers multiply scatter light between deep curved cavities between barbules; inset: jagged barbule margins on some curved array feathers may enhance multiple scattering. (B) Dihedral strap feathers multiply scatter light between the V-shaped barbule arrays and within deep cavities between adjacent barbules. (C) Dense strap feathers form a chaotic array with minimally exposed horizontal surface area, which multiply scatters light. (D) Sparse strap feathers apparently form deep cavities among feathers that produce multi-feather (black, gray, white) scattering. Inset: cross-section of light being multiply scattered between different feathers. (E) Brushy barb feathers multiply scatter light between vertically oriented, simple barbs of multiple densely packed feathers which project vertically from the bird skin.

Journal of Experimental Biology (2019) 222, jeb208140. doi:10.1242/jeb.208140

darker – with significantly flatter reflectance curves (broadband low-reflectance) – than plumages of closely related normal black species (Figs 2 and 3). Melanin pigments absorb shorter wavelengths of light more efficiently, resulting in higher reflectance in the red than the ultraviolet (Meredith and Sarna, 2006). Typically, reflectance curves of black plumage slope upward (Fig. 2A). In contrast, structurally assisted absorption causes plumages to have not only lower overall reflectance but also more uniform reflectance (McCoy et al., 2018). In all cases, the super black plumages described here reflect <2% of light and have a broadband, flat reflectance curve compared with normal black plumages.

In previous work, we analyzed unusual feather microstructures in male bird-of-paradise plumages, which profoundly diminish plumage reflectance through multiple scattering and iterative absorption (McCoy et al., 2018). Likewise, brush-like scales and cuticle microlens arrays in elaborate, brilliantly colored male peacock spiders diminish reflectance and enhance absorption (McCoy et al., 2019). Here, we find that sexual and social selection for profoundly black plumage appearance have resulted in the evolution of five qualitative classes of barbule morphologies: (1) curved arrays, (2) dihedral straps, (3) dense straps, (4) sparse straps and (5) brushy barbs (Figs 5 and 6). Each class of super black feather morphology evolved more than once in multiple avian families (Fig. 4). Quantitative measures of categories 1–4 show that super black feathers are darker if their barbules have cavities in which light is multiply scattered, that is, tightly packed strap-shaped barbules (Fig. 6). We hypothesize that super black evolved through sexual selection because it makes nearby colors (Fig. 1) appear brighter, or even glowing, to observers (Kreezer, 1930; Brainard et al., 1993; Speigle and Brainard, 1996; see Discussion, Super black may enhance nearby color owing to sensory bias).

Microstructures enhance absorption through multiple scattering

Surface structure can collaborate with melanin pigmentation to produce structurally-assisted absorption; with each scattering event, some proportion of incident light is transmitted into the material where it will be absorbed by melanin pigments (Brown et al., 2002; Crouch et al., 2004; Vorobyev et al., 2009; Tao et al., 2012; Liu et al., 2014). Multiple scattering among three-dimensional microscopic surface features much greater in width than wavelengths of visible light thus enhances absorption (Tao et al., 2012). Eumelanin (the pigment molecule in many black bird feathers) has a broadband absorption spectrum (Riesz et al., 2006), with slightly lower absorption at higher wavelengths (Fig. 2). Multiple scattering enhances the absorption efficiency of eumelanin, contributing to lower reflectance and a flatter reflectance curve (Figs 2 and 3). Microscale rough surface features create a velvety, diffuse appearance devoid of specular reflections (Maurer et al., 2017).

Particular structural features of super black feathers minimize exposed horizontal surface area in the viewing direction of an observing individual, but have laminar surfaces oriented vertically to maximize multiple scattering (McCoy et al., 2018). Thus multiple scattering causes iterative melanin-based absorption. These barbule arrays are similar to arrays of razor blades (or other flat objects) that collect stray light (‘beam dumps’; Cadj et al., 1987; Den Hartog

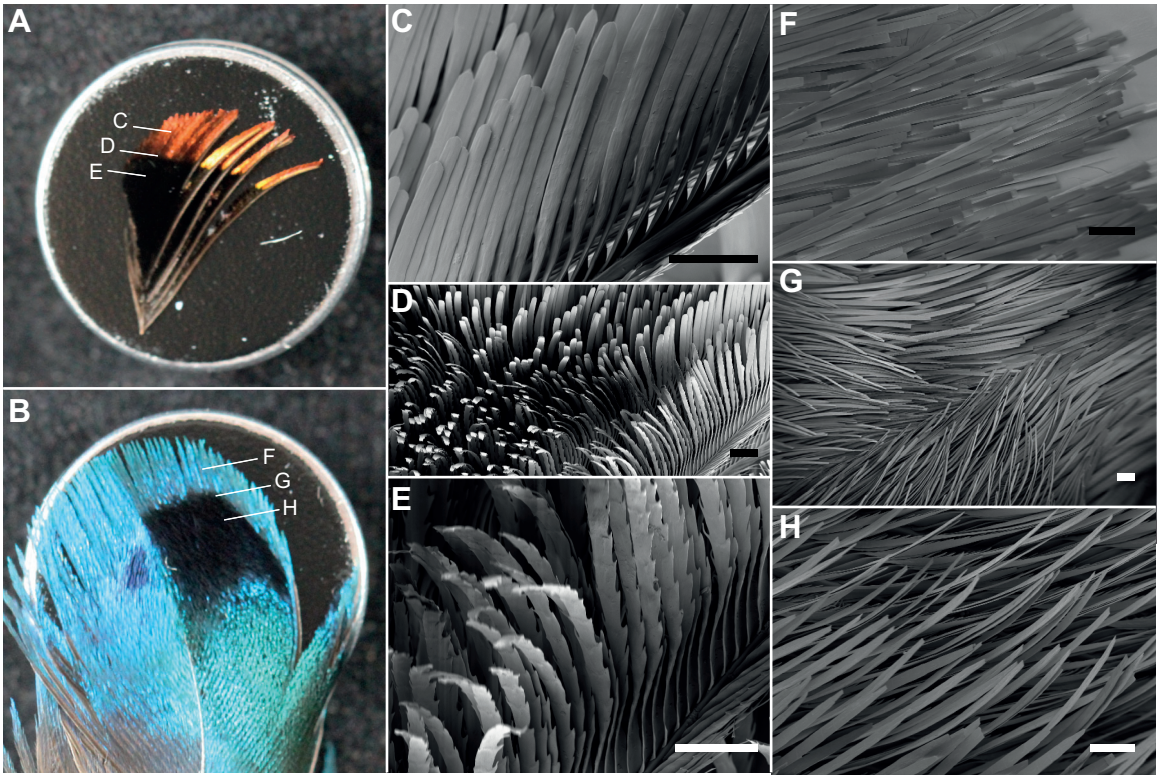

Fig. 8. Barbule morphology varies by color within single feathers in multiple species. Variation in barbule orientation within a single feather of (A,C–E) *Drepanornis bruijnii* (Paradisaeidae) and (B,F–H) *Lamprotornis splendidus* (Sturnidae). (A) *Drepanornis bruijnii* feather mounted on SEM stub. (B) *Lamprotornis splendidus* feather mounted on SEM stub. (C–E) SEM images of *D. bruijnii* corresponding to the letters in A, demonstrating the change in barbule shape and orientation from super black to structurally colored, copper regions. (F–H) SEM images of *L. splendidus* corresponding to the letters in B, demonstrating the change in barbule shape and orientation from super black to copper regions. Diameter of SEM stubs is 12.7 mm; all scale bars are 100 μm.

Journal of Experimental Biology (2019) 222, jeb208140. doi:10.1242/jeb.208140

and Cekic, 1994). Here, quantitative measurements of feather microstructures and a phylogenetic PCA demonstrate that super black feathers separate from normal black feathers owing to (i) how strap-like, rather than cylindrical, the barbules are, and (ii) how tightly packed the barbules are (major components of PC1; Fig. 6A; Dataset S2). The laminar surfaces of strap-like barbules, when they are oriented perpendicularly to the plane of a bird's body, scatter light between the surfaces, causing iterative absorption by melanin. Indeed, PC1 is significantly correlated with reflectance (Fig. 6B,C), supporting this mechanistic conclusion about how super black feathers decrease reflectance through structural effects.

The feathers in the curved array, dihedral strap and dense strap classes enhance absorption through multiple scattering among the barbules of the same barbs (Fig. 7A–C). In contrast, feathers in the sparse strap and brushy barb categories appear to enhance light absorption through multiple scattering among the barbule and ramus surfaces of multiple feathers (Fig. 7D,E). In super black patches of *S. fischeri* and *O. derbianus*, each of these simple brushy feathers is very small, and sticks up vertically from the skin. Together, these arrays of brushy feathers appear to function like the curved arrays of barbules within individual barbs of birds-of-paradise, starlings and fairy-bluebirds (Fig. 7E). Further testing of the hypothesis of multiple scattering among feathers will require examining the 3D structure of microcavities within the intact plumages of the sparse strap and brushy barb type black patches.

The five morphological classes show significant variation in their absorption efficiency, with curved array class feathers having the lowest reflectance – particularly the appropriately named velvet satinbird, *C. loriae*, the Asian fairy-bluebird *I. puella* and the birds-of-paradise – followed by the simple brushy barbs of *S. fischeri* and *O. derbianus*, dihedral strap, dense strap, simple strap and the controls (Spearman's tie-corrected rank correlation, $P<0.0005$). Variations among the independently evolved morphological classes has produced corresponding variation in structural absorption efficiency (Fig. 6A–C). The micro-scale cavities in the curved array barbules are deeper than cavities formed by the other morphological categories, which may make for a more effective light trap.

As predicted by iterative absorption, the spectral shape of many super black reflectance curves resembles the shape of normal black reflectance curves divided by a factor of ∼3–12. Intriguingly, the exceptions to this rule are primarily species with curved array barbules [some birds-of-paradise (Paradiseaidae), the fairy bluebird, *I. puella*, and the duck *N. auritus*], for which the reflectance curves are flatter than normal black reflectance curves of close relative even when divided by an appropriate proportionality factor. Curved array barbules are the most efficient microstructural enhancers of absorption reported here, and further research could focus specifically on microstructural correlates of broadband absorption. Detailed optical simulations would be useful to further explore structural absorption in birds.

Super black occurs near brilliant color in visual displays

All but one of these super black plumage patches are found adjacent to brightly colored plumage patches or fleshy ornaments (Fig. 1, Dataset 1; see discussion of the one exception, *M. alboscapulatus*, below). Super black can frame color, as in *L. superba* (Fig. 1J) and *I. puella* (Fig. 1M), but sometimes super black occurs as small patches inside a colorful scene, as in *S. spectabalis* (Fig. 1A) and *L. superbus* (Fig. 1L). Brilliantly colored peacock spiders also have super black patches within a colorful abdomen (McCoy et al., 2019). Small patches of super black inside colorful plumage look like black holes – dimensionless, profound holes occurring on another plane than the colorful surroundings.

As in birds, the super black wing scales of *Papilio ulysses*, *Troides aeacus* and *Parides sesostris* (Papilionidae) are immediately adjacent to brilliant structurally colored blue, pigmentary yellow and structural green patches, respectively (Vukusic et al., 2004; Zhao et al., 2011b; Wilts et al., 2012). The super black structures of these butterflies may be aposematic signals that have evolved through the sensory biases of avian predators (or they may, too, operate in mate choice). In peacock spiders, the super black cuticle and scales of *Maratus speciosus* and *Maratus karrie* are adjacent to brilliant blue and red patches, and are prominently featured during extended mating displays (Otto and Hill, 2012, 2014).

Most of the normal black, control species lacked vivid color patches, but the few exceptions are instructive. For example, like most other subspecies, *Lepitothrix coronata coronata* has a vivid blue crown with normal black body plumage. But the Central American subspecies, *L. c. velutina*, combines super black body plumage with a similar blue crown (Fig. 1D). Thus, super black body plumage evolved uniquely in *L. c. velutina* after the origin of the vividly blue crown and normal black plumage in the common ancestor of *Lepitothrix coronata*, as the sensory bias hypothesis predicts. A parallel evolutionary pattern is also exhibited by the manakin *Masius chrysopterus pax* compared with other subspecies.

One bird has super black plumage without adjacent colorful patches: *M. alboscapulatus* has super black body plumage combined with white epaulets. However, we found that super black plumage is shared by, and primitive to, all *Malurus* species, and likely evolved in the most recent common ancestor of the genus in combination with brilliant structural blue coloration (Fig. 2). Thus, *M. alboscapulatus* – the brightest super black bird in our sample – has retained super black plumage despite having lost saturated blue feathers and evolved bright white patches.

Super black may enhance nearby color owing to sensory bias

We propose that super black is an optical illusion for color emphasis. Super black in visual display is found adjacent to bright colors (see Discussion, Super black occurs near brilliant color in visual displays). We hypothesize that, as in birds-of-paradise (McCoy et al., 2018) and brilliantly colored peacock spiders (McCoy et al., 2019), super black plumage patches enhance the perceived brilliance of adjacent patches of saturated colors owing to a sensory/cognitive bias intrinsic to color vision in variable light environments. Vertebrates use white, specular highlights across the visual scene to estimate, and control for, variation in ambient light intensity and spectral composition (Brainard et al., 1993). In this manner, the observer creates color perceptions that do not fluctuate freely with variation in ambient light conditions. Dark black surfaces eliminate the specular highlights that provide local information about the quantity of ambient light illuminating the visual scene. When a colored surface is reflecting more light than the observer estimates is ambient on it, then the surfaces may appear 'self-luminous'– i.e. as if emitting their own light – or appear to 'pop' out from the surface (Hering, 1879; Kreezer, 1930; Brainard et al., 1993; Speigle and Brainard, 1996). Super black will not make adjacent white surfaces appear brighter because white surfaces themselves provide visual information about the magnitude and quality of ambient illumination (Hering, 1879; Kreezer, 1930; Speigle and Brainard, 1996).

Evidence of the use of specular reflections for color correction has been found in goldfish and humans (Speigle and Brainard,

1996; Neumeyer et al., 2002; Bach and Poloschek, 2006). Thus, we hypothesize that this neural mechanism for color correction evolved in the most recent common ancestor of all bony vertebrates, and created an enduring, systemic sensory/cognitive bias that has influenced the evolution of ornamental sexual and social signals within birds. Sensory and cognitive biases have been proposed to influence signal perception owing to an observer's underlying sensory physiology or cognitive mechanisms (Ryan, 1990; Ryan and Rand, 1990; Endler and Basolo, 1998; Rosenthal and Evans, 1998; Basolo, 2002). Super black plumage adjacent to bright color appears to be an example of evolution by sensory bias. Recently, we have shown that some peacock spiders (*Maratus* sp.) have also evolved super black near brilliant color patches used in sexual displays (McCoy et al., 2019). Although mechanistically dissimilar from that of vertebrates (Zurek et al., 2015), color vision in peacock spiders may share the same color correction mechanism, leading to this sensory bias.

We do not yet have experimental confirmation of the effect of super black on mechanisms of color correction in birds. It is important to note, however, that the discovery of massively parallel evolution of super black plumage patches adjacent to brilliant, saturated colors that function in communication is, by itself, evidence of a sensory/cognitive bias in multiple independent lineages of birds. Further research is required to investigate this mechanistic basis behind this bias.

Acknowledgements
We thank the Yale Peabody Museum of Natural History, the American Museum of Natural History and the Harvard Museum of Comparative Zoology for research use of ornithological specimens. We are grateful to Kristof Zyskowski, Jeremiah Trimble, Kate Eldridge and Arthur McClelland for help selecting and imaging specimens. David Haig provided useful feedback.

Competing interests
The authors declare no competing or financial interests.

Author contributions
Conceptualization: D.E.M., R.O.P.; Methodology: D.E.M., R.O.P.; Software: D.E.M.; Validation: D.E.M., R.O.P.; Formal analysis: D.E.M.; Investigation: D.E.M.; Resources: D.E.M., R.O.P.; Data curation: D.E.M., R.O.P.; Writing - original draft: D.E.M., R.O.P.; Writing - review & editing: D.E.M., R.O.P.; Visualization: D.E.M., R.O.P.; Supervision: R.O.P.; Project administration: R.O.P.; Funding acquisition: D.E.M., R.O.P.

Funding
This work was performed in part at the Harvard University Center for Nanoscale Systems (CNS), a member of the National Nanotechnology Coordinated Infrastructure Network (NNCI), which is supported by the National Science Foundation under NSF ECCS award no. 1541959. D.E.M.'s research is conducted with Government support under and awarded by the Department of Defense, Army Research Office, National Defense Science and Engineering Graduate (NDSEG) Fellowship, 32 CFR 168a. D.E.M. is also supported by a Theodore H. Ashford Graduate Fellowship. The research was supported by the William Robertson Coe Fund of Yale University.

Supplementary information
Supplementary information available online at
http://jeb.biologists.org/lookup/doi/10.1242/jeb.208140.supplemental

References
Bach, M. and Poloschek, C. M. (2006). Optical illusions. *Adv. Clin. Neurosci. Rehabil.* **6**, 20-21.
Basolo, A. L. (2002). Congruence between the sexes in preexisting receiver responses. *Behav. Ecol.* **13**, 832-837. doi:10.1093/beheco/13.6.832
Brainard, D. H., Wandell, B. A. and Chichilnisky, E.-J. (1993). Color constancy: from physics to appearance. *Curr. Dir. Psychol. Sci.* **2**, 165-170. doi:10.1111/1467-8721.ep10769003
Brown, R. J. C., Brewer, P. J. and Milton, M. J. T. (2002). The physical and chemical properties of electroless nickel–phosphorus alloys and low reflectance nickel–phosphorus black surfaces. *J. Mater. Chem.* **12**, 2749-2754. doi:10.1039/B204483H
Cadj, F. M., Cheever, D. R., Klicker, K. A. and Stover, J. C. (1987). Comparison of scatter data from various beam dumps. In *Current Developments in Optical Engineering II* (ed. R. E. Fischer, W. J. Smith), pp. 21-25. International Society for Optics and Photonics.
Crouch, C. H., Carey, J. E., Warrender, J. M., Aziz, M. J., Mazur, E. and Génin, F. Y. (2004). Comparison of structure and properties of femtosecond and nanosecond laser-structured silicon. *Appl. Phys. Lett.* **84**, 1850-1852. doi:10.1063/1.1667004
Den Hartog, D. J. and Cekic, M. (1994). A simple, high-performance Thomson-scattering diagnostic for high-temperature plasma research. *Meas. Sci. Technol.* **5**, 1115. doi:10.1088/0957-0233/5/9/013
Endler, J. A. and Basolo, A. L. (1998). Sensory ecology, receiver biases and sexual selection. *Trends Ecol. Evol.* **13**, 415-420. doi:10.1016/S0169-5347(98)01471-2
Felsenstein, J. (1985). Phylogenies and the comparative method. *Am. Nat.* **125**, 1-15. doi:10.1086/284325
Frith, D. W. and Frith, C. W. (1988). Courtship display and mating of the superb bird of paradise *Lophorina superb*. *Emu* **88**, 183-188. doi:10.1071/MU9880183
Grafen, A. (1989). The phylogenetic regression. *Philos. Trans. R. Soc. B* **326**, 119-157. doi:10.1098/rstb.1989.0106
Harvey, T. A., Bostwick, K. S. and Marschner, S. (2013). Directional reflectance and milli-scale feather morphology of the African emerald cuckoo, *Chrysococcyx cupreus*. *J. R. Soc. Interface* **10**, 20130391. doi:10.1098/rsif.2013.0391
Hering, E. (1879). Der Raumsinn Und Die Bewegungen Des Auges. *Handbuch der Physiologie* (ed. L. Hermann). Leipzig: FCW Vogel.
Hill, G. E. and McGraw, K. J. (2006). *Bird Coloration: Function and Evolution*. Cambridge: Harvard University Press.
Iskandar, J.-P., Eliason, C. M., Astrop, T., Igic, B., Maia, R. and Shawkey, M. D. (2016). Morphological basis of glossy red plumage colours. *Biol. J. Linn. Soc.* **119**, 477-487. doi:10.1111/bij.12810
Jetz, W., Thomas, G. H., Joy, J. B., Hartmann, K. and Mooers, A. O. (2012). The global diversity of birds in space and time. *Nature* **491**, 444-448. doi:10.1038/nature11631
Jetz, W., Thomas, G. H., Joy, J. B., Redding, D. W., Hartmann, K. and Mooers, A. O. (2014). Global distribution and conservation of evolutionary distinctness in birds. *Curr. Biol.* **24**, 919-930. doi:10.1016/j.cub.2014.03.011
Kreezer, G. (1930). Luminous appearances. *J. Gen. Psychol.* **4**, 247-281. doi:10.1080/00221309.1930.9918313
Liu, X., Coxon, P. R., Peters, M., Hoex, B., Cole, J. M. and Fray, D. J. (2014). Black silicon: fabrication methods, properties and solar energy applications. *Energy Environ. Sci.* **7**, 3223-3263. doi:10.1039/C4EE01152J
Martins, E. P. and Hansen, T. F. (1997). Phylogenies and the comparative method: a general approach to incorporating phylogenetic information into the analysis of interspecific data. *Am. Nat.* **149**, 646-667. doi:10.1086/286013
Maurer, D. L., Kohl, T. and Gebhardt, M. J. (2017). Cuticular microstructures turn specular black into matt black in a stick insect. *Arthropod. Struct. Dev.* **46**, 147-155. doi:10.1016/j.asd.2016.11.006
McCoy, D. E., Feo, T., Harvey, T. A. and Prum, R. O. (2018). Structural absorption by barbule microstructures of super black bird of paradise feathers. *Nat. Commun.* **9**, 1-8. doi:10.1038/s41467-017-02088-w
McCoy, D. E., McCoy, V. E., Mandsberg, N. K., Shneidman, A. V., Aizenberg, J., Prum, R. O. and Haig, D. (2019). Structurally assisted super black in colourful peacock spiders. *Proc. R. Soc. B* **286**, 20190589. doi:10.1098/rspb.2019.0589
Meredith, P. and Sarna, T. (2006). The physical and chemical properties of eumelanin. *Pigment Cell Res.* **19**, 572-594. doi:10.1111/j.1600-0749.2006.00345.x
Neumeyer, C., Dörr, S., Fritsch, J. and Kardelky, C. (2002). Colour constancy in goldfish and man: influence of surround size and lightness. *Perception* **31**, 171-188. doi:10.1068/p05sp
Otto, J. C. and Hill, D. E. (2012). Notes on *Maratus* Karsch 1878 and related jumping spiders from Australia, with five new species (Araneae: Salticidae: Euophryinae). *Peckhamia* **103**, 1-81. doi:10.11646/zootaxa.4564.1.3
Otto, J. C. and Hill, D. E. (2014). Spiders of the mungaich group from Western Australia (Araneae: Salticidae: Euophryinae: Maratus), with one new species from Cape Arid. *Peckhamia* **112**, 1-35. doi:10.18195/issn.0312-3162.29(2).2014.149-158
Panagiotopoulos, N. T., Diamanti, E. K., Koutsokeras, L. E., Baikousi, M., Kordatos, E., Matikas, T. E., Gournis, D. and Patsalas, P. (2012). Nanocomposite catalysts producing durable, super-black carbon nanotube systems: applications in solar thermal harvesting. *ACS Nano* **6**, 10475-10485. doi:10.1021/nn304531k
Prum, R. O. (2006). Anatomy, physics, and evolution of avian structural colors. In: *Bird Coloration. Vol. 1: Mechanisms and Measurements* (ed. G. E. Hill, K. J. McGraw), pp. 295-353. Harvard University Press.
Prum, R. O. and Razafindratsita, V. R. (1997). Lek behavior and natural history of the velvet asity (*Philepitta castanes*: Eurylaimidae). *Wilson Bull.* **109**, 371-392.
Revell, L. J. (2009). Size-correction and principal components for interspecific comparative studies. *Evolution* **63**, 3258-3268. doi:10.1111/j.1558-5646.2009.00804.x
Revell, L. J. (2012). phytools: an R package for phylogenetic comparative biology (and other things). *Methods Ecol. Evol.* **3**, 217-223. doi:10.1111/j.2041-210X.2011.00169.x

Revell, L. J. (2013). Two new graphical methods for mapping trait evolution on phylogenies. *Methods Ecol. Evol.* **4**, 754-759. doi:10.1111/2041-210X.12066
Riesz, J., Gilmore, J. and Meredith, P. (2006). Quantitative scattering of melanin solutions. *Biophys. J.* **90**, 4137-4144. doi:10.1529/biophysj.105.075713
Rosenthal, G. G. and Evans, C. S. (1998). Female preference for swords in *Xiphophorus helleri* reflects a bias for large apparent size. *Proc. Natl. Acad. Sci. USA* **95**, 4431-4436. doi:10.1073/pnas.95.8.4431
Rubolini, D., Liker, A., Garamszegi, L. Z., Møller, A. P. and Saino, N. (2015). Using the BirdTree.org website to obtain robust phylogenies for avian comparative studies: a primer. *Curr. Zool.* **61**, 959-965. doi:10.1093/czoolo/61.6.959
Ryan, M. J. (1990). Sexual selection, sensory systems and sensory exploitation. *Oxford Surv. Evol. Biol.* **7**, 157-195.
Ryan, M. J. and Rand, A. S. (1990). The sensory basis of sexual selection for complex calls in the túngara frog, *Physalaemus pustulosus* (sexual selection for sensory exploitation). *Evolution* **44**, 305-314. doi:10.1111/j.1558-5646.1990.tb05200.x
Scholes, E. (2008). Structure and composition of the courtship phenotype in the bird of paradise *Parotia lawesii* (Aves: Paradisaeidae). *Zoology* **111**, 260-278. doi:10.1016/j.zool.2007.07.012
Scholes, E. and Laman, T. G. (2018). Distinctive courtship phenotype of the Vogelkop superb bird-of-paradise *Lophorina niedda* Mayr, 1930 confirms new species status. *PeerJ* **6**, e4621. doi:10.7717/peerj.4621
Shawkey, M. D. and D'Alba, L. (2017). Interactions between colour-producing mechanisms and their effects on the integumentary colour palette. *Philos. Trans. R. Soc. B* **372**, 20160536. doi:10.1098/rstb.2016.0536
Speigle, J. M. and Brainard, D. H. (1996). Luminosity thresholds: effects of test chromaticity and ambient illumination. *JOSA A* **13**, 436-451. doi:10.1364/JOSAA.13.000436
Spinner, M., Kovalev, A., Gorb, S. N. and Westhoff, G. (2013). Snake velvet black: hierarchical micro- and nanostructure enhances dark colouration in *Bitis rhinoceros*. *Sci. Rep.* **3**, 1846. doi:10.1038/srep01846
Stavenga, D. G., Leertouwer, H. L., Marshall, N. J. and Osorio, D. (2011). Dramatic colour changes in a bird of paradise caused by uniquely structured breast feather barbules. *Proc. R. Soc. B Biol. Sci.* **278**, 2098-2104. doi:10.1098/rspb.2010.2293
Stavenga, D. G., Leertouwer, H. L., Osorio, D. C. and Wilts, B. D. (2015). High refractive index of melanin in shiny occipital feathers of a bird of paradise. *Light Sci. Appl.* **4**, e243. doi:10.1038/lsa.2015.16
Stoddard, M. C. and Prum, R. O. (2011). How colorful are birds? Evolution of the avian plumage color gamut. *Behav. Ecol.* **22**, 1042-1052. doi:10.1093/beheco/arr088
Tao, H., Lin, J., Hao, Z., Gao, X., Song, X., Sun, C. and Tan, X. (2012). Formation of strong light-trapping nano- and microscale structures on a spherical metal surface by femtosecond laser filament. *Appl. Phys. Lett.* **100**, 201111. doi:10.1063/1.4719108
Vorobyev, A. Y., Topkov, A. N., Gurin, O. V., Svich, V. A. and Guo, C. (2009). Enhanced absorption of metals over ultrabroad electromagnetic spectrum. *Appl. Phys. Lett.* **95**, 121106. doi:10.1063/1.3227668
Vukusic, P., Sambles, J. R. and Lawrence, C. R. (2004). Structurally assisted blackness in butterfly scales. *Proc. R. Soc. London. Ser. B Biol. Sci.* **271**, S237-S239. doi:10.1098/rsbl.2003.0150
Wilts, B. D., Michielsen, K., De Raedt, H. and Stavenga, D. G. (2012). Iridescence and spectral filtering of the gyroid-type photonic crystals in *Parides sesostris* wing scales. *Interface Focus* **2**, 681-687. doi:10.1098/rsfs.2011.0082
Wilts, B. D., Michielsen, K., De Raedt, H. and Stavenga, D. G. (2014). Sparkling feather reflections of a bird-of-paradise explained by finite-difference time-domain modeling. *Proc. Natl. Acad. Sci. USA* **111**, 4363-4368. doi:10.1073/pnas.1323611111
Zhao, Q., Fan, T., Ding, J., Zhang, D., Guo, Q. and Kamada, M. (2011a). Super black and ultrathin amorphous carbon film inspired by anti-reflection architecture in butterfly wing. *Carbon N. Y.* **49**, 877-883. doi:10.1016/j.carbon.2010.10.048
Zhao, Q., Guo, X., Fan, T., Ding, J., Zhang, D. and Guo, Q. (2011b). Art of blackness in butterfly wings as natural solar collector. *Soft Mat.* **7**, 11433-11439. doi:10.1039/c1sm06167d
Zurek, D. B., Cronin, T. W., Taylor, L. A., Byrne, K., Sullivan, M. L. G. and Morehouse, N. I. (2015). Spectral filtering enables trichromatic vision in colorful jumping spiders. *Curr. Biol.* **25**, R403-R404. doi:10.1016/j.cub.2015.03.033

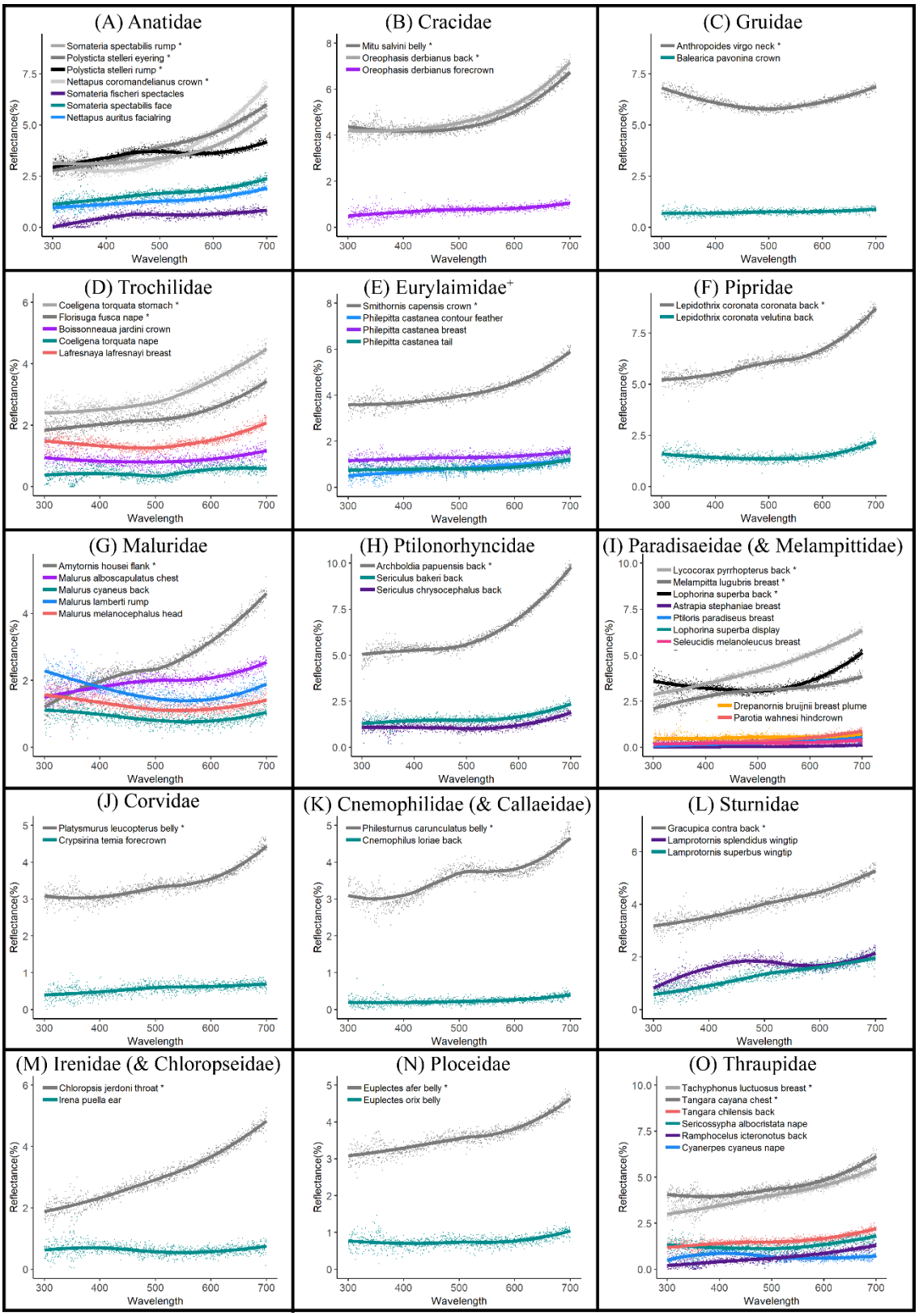

Figure S1. Complete spectrophotometry results. Directional reflectance is shown at 90˚ incidence. Spectra of control species and patches are labeled with an *, and shown in gray scale; super black patches are shown in color. This figure refers to Fig. 2.

[+]note on Eurylaimidae: contour feather is the black base of a newly molted, green-tipped contour feather

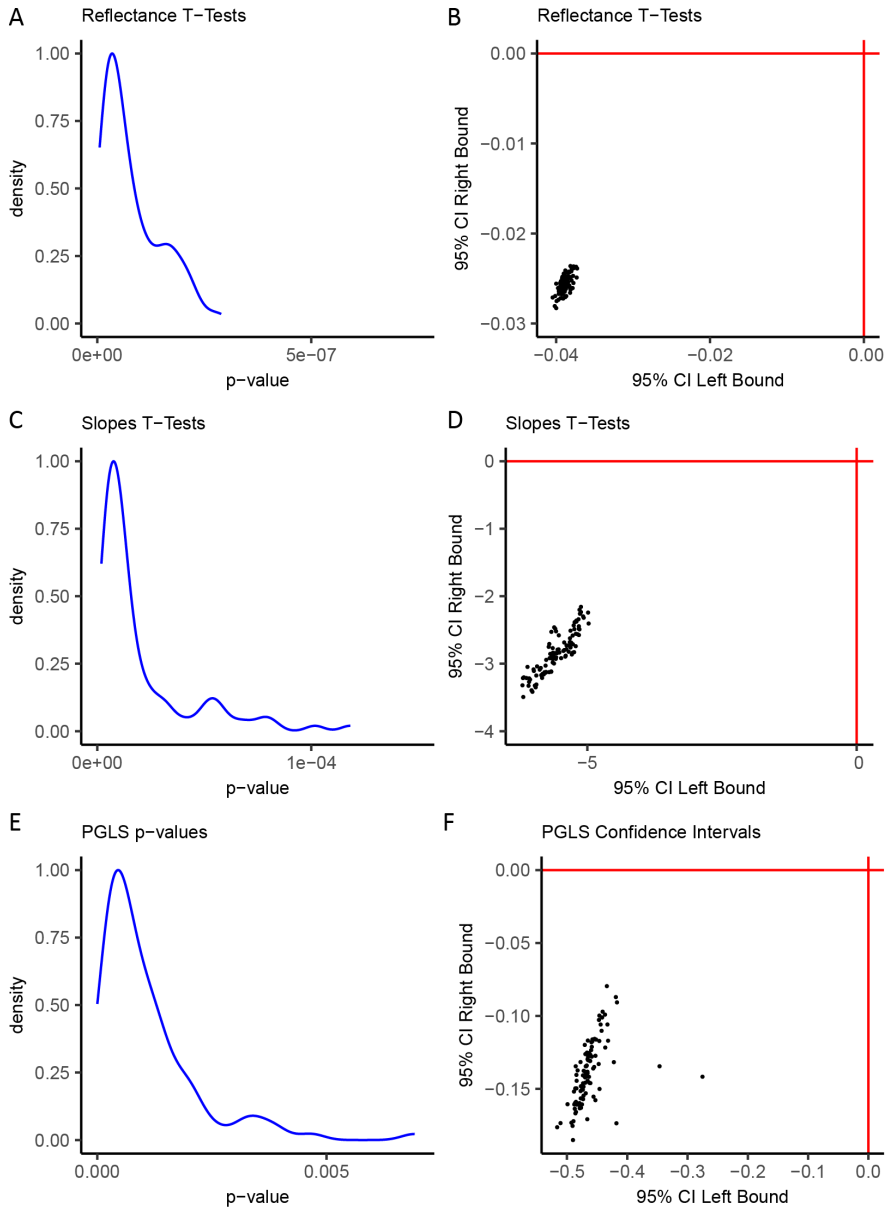

Figure S2: P-values were significant and confidence intervals did not include 0 for all statistical tests. (A-B) Reflectance t-tests (super black feathers are darker than normal black); **(C-D)** Slopes t-tests (super black feathers have a flatter, more broadband reflectance curve than normal black feathers); **(E-F)** PGLS between PC1 and reflectance (microstructure is correlated with reflectance). **(A)** P-values for 100 repetitions of t-tests comparing normal, directional reflectance of super black to control black birds. **(B)** 95% confidence intervals for 100 repetitions of t-tests comparing normal, directional reflectance of super black to control black birds. **(C)** P-values for 100 repetitions of t-tests comparing normal, directional reflectance curve best-fit slopes of super black to control black birds. **D)** 95% confidence intervals for 100 repetitions of t-tests comparing normal, directional reflectance curve best-fit slopes of super black to control black birds. **(E)** P-values were less than 0.05 for all 100 PGLS models comparing PC1 and reflectance (each model sampled from a different tree). **(F)** Confidence intervals did not include 0 in any of the 100 PGLS models comparing PC1 and reflectance (each model sampled from a different tree). Red lines are at right or left bound = 0. **(A-D)** refer to Fig. 3; **(E-F)** refer to Fig. 6.

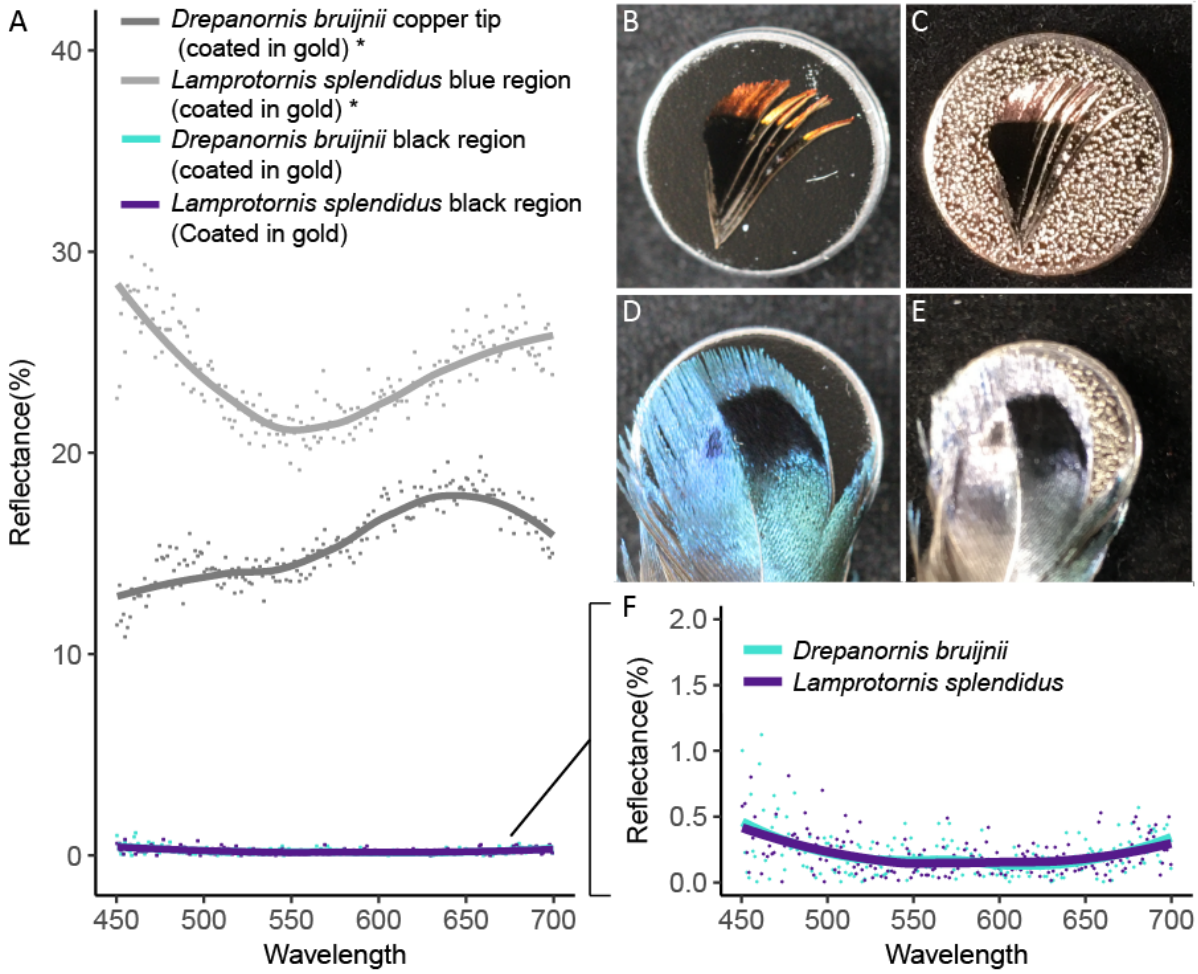

Figure S3: Even after being coated in gold, structurally absorbent feathers reflect <0.5% of directionally incident light. (A) Normal, directional reflectance spectra for individual, gold-coated feathers of *Drepanornis bruijnii* and *Lamprotornis splendidus*. Black regions and structurally colored regions are both plotted. Inset: **(B)** *Drepanornis bruijnii* feather mounted but uncoated. **(C)** *Drepanornis bruijnii* feather mounted and coated in ~15 nm gold. **(D)** *Lamprotornis splendidus* wingtip feather mounted but uncoated. **(E)** *Lamprotornis splendidus* wingtip feather mounted and coated in gold. Diameter of SEM stubs in each photo is 12.7 mm. **(F)** Zoomed-in reflectance spectra of super black regions of *Drepanornis bruijnii* and *Lamprotornis splendidus*

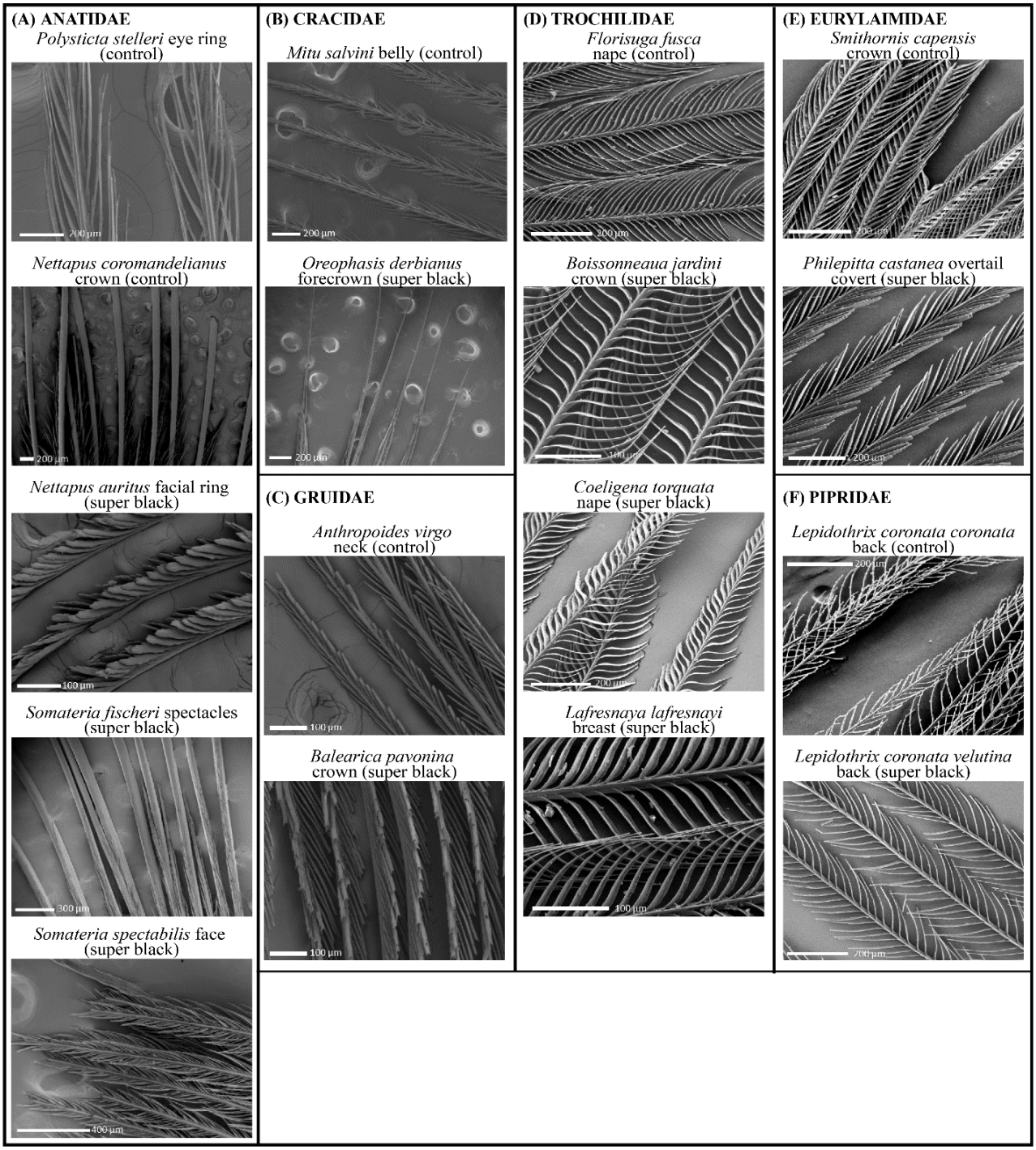

Figure S4: Representative SEM photos: part one of three. (**A**) Anatidae. (**B**) Cracidae. (**C**) Gruidae. (**D**) Trochilidae. (**E**) Eurylaimidae. (**F**) Pipridae. Additional magnifications and high-resolution micrographs are available online on the Dryad repository. See Figures S5-S6 for remaining families.

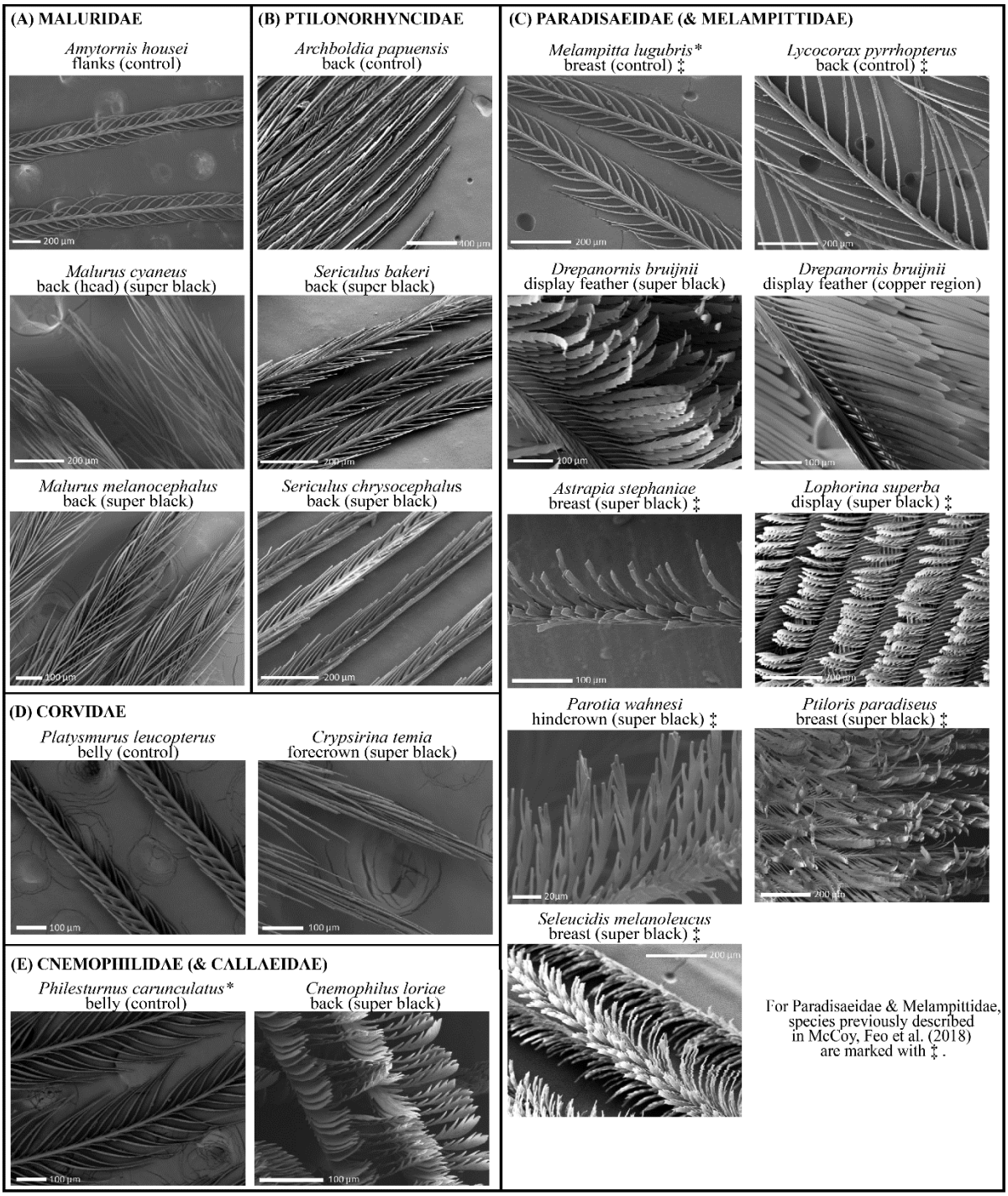

Figure S5: Representative SEM photos: part two of three. (**A**) Maluridae. (**B**) Ptilonorhynchidae. (**C**) Paradisaeidae (& Melampittidae). (**D**) Corvidae. (**E**) Cnemophilidae (& Callaeidae). Additional magnifications and high-resolution micrographs are available online on the Dryad repository. See Figures S4, S6 for remaining families. *indicates a species who belongs to the family in parentheses.

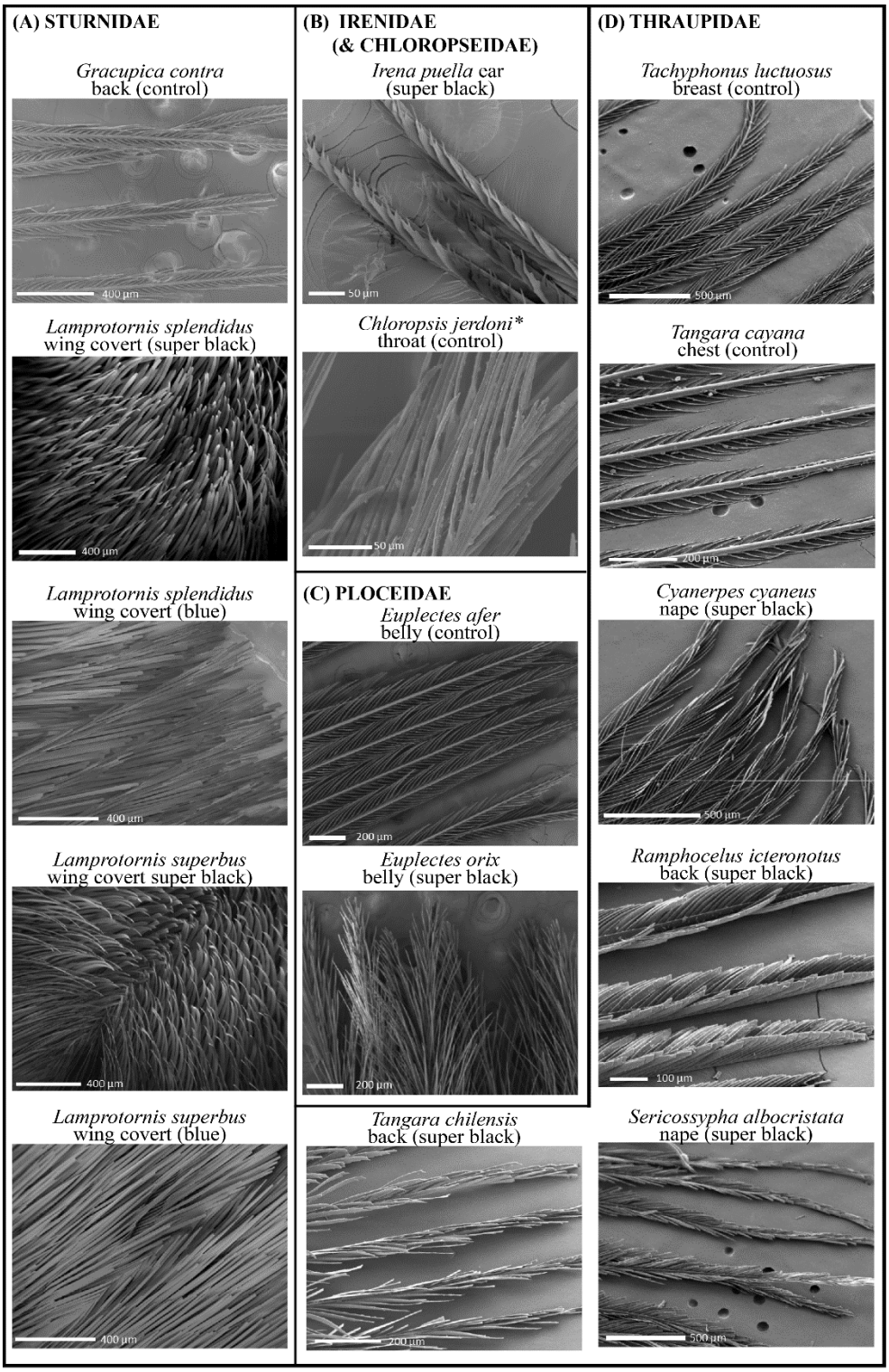

Figure S6: Representative SEM photos: part three of three. (A) Sturnidae. (**B**) Irenidae (& Chloropseidae). (**C**) Ploceidae. **(D)** Thraupidae. Additional magnifications and high-resolution micrographs are available online on the Dryad repository. See Figures S4-S5 for remaining families. *indicates a species who belongs to the family in parentheses.

Dataset S1: Specimen information, barbule categories, and reflectance.

Click here to Download Dataset S1

Dataset S2: PCA loadings and PC1 scores for the phylogenetic PCA.

Click here to Download Dataset S2